Diagnostic Atlas of

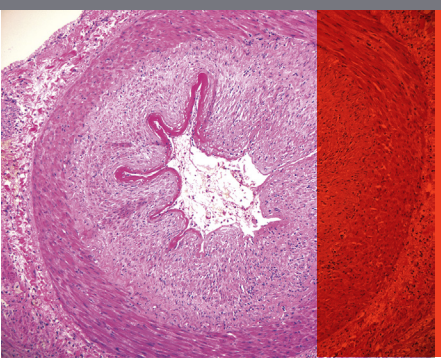

RENAL PATHOLOGY

3rd Edition

Agnes B. Fogo, MD

John L. Shapiro Professor of Pathology
Professor of Medicine and Pediatrics
Director, Renal/Electron Microscopy Laboratory
Department of Pathology, Microbiology and Immunology
Vanderbilt University Medical Center
Nashville, Tennessee

Michael Kashgarian, MD

Professor Emeritus of Pathology and Molecular, Cellular, and Developmental Biology
Department of Pathology
Yale University
New Haven, Connecticut

ELSEVIER

ELSEVIER

1600 John F. Kennedy Blvd.
Ste 1800
Philadelphia, PA 19103-2899

DIAGNOSTIC ATLAS OF RENAL PATHOLOGY, THIRD EDITION ISBN: 978-0-323-39053-8

Library of Congress Cataloging-in-Publication Data

Names: Fogo, Agnes B., author. | Kashgarian, Michael, author.
Title: Diagnostic atlas of renal pathology / Agnes B. Fogo, Michael Kashgarian.
Description: 3rd edition. | Philadelphia, PA : Elsevier, [2017] | Includes bibliographical references and index.
Identifiers: LCCN 2016033251 | ISBN 9780323390538 (hardcover : alk. paper)
Subjects: | MESH: Kidney Diseases--diagnosis | Kidney Diseases--pathology | Atlases
Classification: LCC RC903 | NLM WJ 17 | DDC 616.6/1--dc23
LC record available at https://lccn.loc.gov/2016033251

Content Strategist: Maureen Iannuzzi
Senior Content Development Specialist: Janice M. Gaillard
Publishing Services Manager: Catherine Jackson
Senior Project Manager: Daniel Fitzgerald
Designer: Renee Duenow
Art and Illustration Buyer: Emily Costantino
Marketing Manager: Michele Milano

Printed in China

Last digit is the print number: 9 8 7 6 5 4 3 2 1

Preface

In the 5 years since our second edition was published, there have been many advances in the genetics, etiology, pathogenesis, and treatment of medical renal diseases. These advances have led to a therapeutic focus on a more specific and personalized approach and, in turn, further emphasized the importance and central role of the renal biopsy in patient management. We have taken these factors into consideration in organizing and adding new material for the third edition of this renal pathology textbook. The organization of this edition follows that of the previous editions, with each of the sections being expanded and updated to include new classifications of various kidney diseases, both native and transplant related. In addition, we have added new chapters. First, we have added an integrative approach to analyzing the findings observed in the kidney biopsy, integrating light microscopy with immunofluorescence and electron microscopy findings. The approach is illustrated as algorithms and Venn diagrams, which together show pathways to diagnoses and the overlap observed for selected morphologic lesions. We have also added a section on endemic nephropathies, an important worldwide challenge. Improved detection and specific diagnosis will be important to begin to identify the common and varying underlying etiologies of this group of diseases. Sections on genetics, etiology, and pathogenesis have also been expanded. References have been updated and continue to be focused, rather than encyclopedic, with emphasis on classic and most recent literature on each subject.

Because this is primarily an atlas, we have added numerous new images. These include illustrations of additional entities and expanded illustrations of the spectrum of lesions present in diseases already included in the previous edition and updated differential diagnosis and key diagnostic features tables for each section. A new feature in the online version is the use of overlays to decode selected electron microscopic images to enhance understanding of the components of the lesions. Together with the numerous images and focused text, this atlas thus provides in-depth and detailed illustrations of a large spectrum of morphologic lesions encountered in the renal biopsy and an approach to differential diagnosis and key prognostic, pathogenetic, and etiologic information.

Agnes B. Fogo
Michael Kashgarian

Acknowledgments

Renal pathology is an exciting process of integrating complex information, relying on a team of nephrologists, pathologists, and highly skilled laboratory personnel. Similar teamwork has gone into the preparation of this book. The deep satisfaction derived from the previous editions of our atlas, along with ongoing advances and realizations that we could further update and enhance our presentation of renal pathology in a usable and concise format, have led to this third edition. The ongoing dedication and partnership with Dr. Michael Kashgarian have been essential to the success of our project. I would also like to thank my renal pathology laboratory team, my fellows and colleagues, who have been essential for this work. I continue to be grateful to my past fellows, especially Drs. Paisit Paueksakon, Xochi Geiger, Patricia Revelo, Michele Rossini, Aruna Dash, and Huma Fatima, and more recent fellows, including Drs. Mark Lusco, Elizabeth Martinez, and Paul Persad, who have searched and hunted for the most instructive and beautiful examples of lesions to expand this atlas. I am also indebted to the expert help of Brent Weedman for imaging and photography assistance.

Lastly, I would like to thank my husband, Byron, and my children, Katherine, Michelle, and Kristin, for their enthusiastic support and encouragement for all of my endeavors.

Agnes B. Fogo

This third edition follows our commitment to present medical renal pathology in a form that is accessible to a wide audience. We have used the lessons learned from the residents, fellows, and colleagues who have commented on our previous work in presenting the expansion of knowledge in this field. As such, it reflects a maturation of our discipline over the past 50 years that began with the contributions of the early pioneers of renal pathology, Robert Heptinstall, Conrad Pirani, Jacob Churg, Ben Spargo, and Robert McCluskey. I am indebted to the many clinical colleagues that I have had the pleasure of working with during these formative years of renal pathology. Their constant queries about the relative importance of specific features of individual biopsies in determining clinical outcomes has led us to incorporate their clinical approaches into our analysis of what we see under the microscope. I would also like to dedicate this work to those who initially started me on the path of studying the kidney. Franklin Epstein was the first to introduce me to the wonders and complexity of the physiology of the kidney. Karl Ullrich taught me the scientific methods and tools necessary to investigate them. Averill Liebow inspired me to pursue pathology as a career. The field of renal pathology was in its infancy when I began my career, and it was the encouragement of these mentors and early pioneers in the field that kept me focused on this discipline. My recent fellows (Matt Palmer, Ekaterina Castano, Liying Fu, and Aaron Hartman) have assisted in many ways not only in the search of the best examples for publication but also in constantly maintaining a dialogue rather than accepting without question my pontifications. The expert help of my administrative assistant and the staffs of the Yale Pathology Graphics and Imaging and Histology sections was essential to the preparation of the images and the manuscript. Finally, I would like to thank my wife, Jean, for her patience and encouragement as I prepared this work.

Michael Kashgarian

Approach to Diagnosis of the Kidney Biopsy

CHAPTER 1

The approach to diagnosing disease in renal biopsy specimens requires information from several different sources to be integrated into a single interpretation: The sources include the clinical data, and examination by light microscopy, immunohistology, and electron microscopy. Each of the sources has several individual variables that must be either included or dismissed in the final evaluation. George Boole in his books *The Mathematical Analysis of Logic* (1847) and *An Investigation of the Laws of Thought* (1854) introduced a branch of algebra in which the values of the variables are the truth values *true* and *false,* usually denoted 1 and 0, respectively, the basis of our current digital world. This expanded the range of applications that can be handled from propositions having only two potential values to those having many. Thus in many ways, the complex analysis of the renal biopsy findings leading to a diagnosis can be viewed as an exercise in Boolean logic.

From the clinical and laboratory data, a decision must be made whether the disease process is acute or chronic; whether it is tubular or interstitial disease, vascular disease or glomerular disease, or a combination of any of these. If there are glomerular lesions, are they proliferative, necrotizing or sclerosing? If there is no proliferation, we must determine by immunofluorescence whether immunoglobulins and/or complement deposits are present or not. If no immunoglobulins or complement deposits are seen, we must determine by electron microscopy whether podocytes are extensively effaced or not. At each step we make a true or false decision and form a lattice (ie, *algorithm* or *schema,* Figs. 1.1–1.4) to narrow our diagnostic choices. Alternatively, sets of decisions are made with the variables of each of the biopsy sources of information (ie, light microscopy, immunohistology, and electron microscopy) forming separate overlapping Boolean logic circles (Figs. 1.5 and 1.6). Finally each of the lattices or circles can be superimposed and their intersections used to arrive at a final interpretation or diagnosis.

For glomerular diseases the pattern of injury by light microscopy should be specified (Table 1.1), for example, mesangial versus endocapillary hypercellularity, or necrosis, crescents, or sclerosis, noting that mixed patterns of glomerular injury often coexist. If immunoglobulins are present, the localization and pattern of deposition, for example, peripheral capillary, mesangial, or both (Table 1.2), should be noted. On ultrastructural examination, changes should be noted in each of the cell types, for example, podocytes, endothelial cells, and mesangial cells, as well as the basement membranes, mesangial matrix, and tubulointerstitium (Table 1.3). The final diagnosis is made based on the presence or absence of a convergence of all of these findings.

If the process predominantly involves the tubulointerstitium (Table 1.4), we must determine whether the process is acute or chronic. Disproportionate increase in interstitial inflammatory cells indicates a tubulointerstitial nephritis, with edema in acute interstitial nephritis and fibrosis and atrophy of tubules in chronic interstitial nephritis. Possible specific underlying etiologies are then assessed; for example, assessing for monoclonal light chain casts, viral inclusions, or evidence of deposits.

Arteriosclerosis with intimal and medial thickening of arteries is typical in any chronic kidney disease, but vascular lesions may also be the primary abnormality underlying renal dysfunction. Thrombosis, necrosis, vasculitis, and cholesterol emboli are examples of specific vascular lesions associated with specific diagnoses (Table 1.5).

Systematic assessment of each of these anatomic compartments, and integration of each modality of tissue examination with the clinical history then allows a specific diagnosis to be made. Ideally, a disease entity/pathogenic type (if disease entity is not known) is diagnosed. Lastly, specific scoring/grading/classification may be applied to arrive at a complete clinicopathologic diagnosis, driven by a logical pathogenic/etiologic approach.

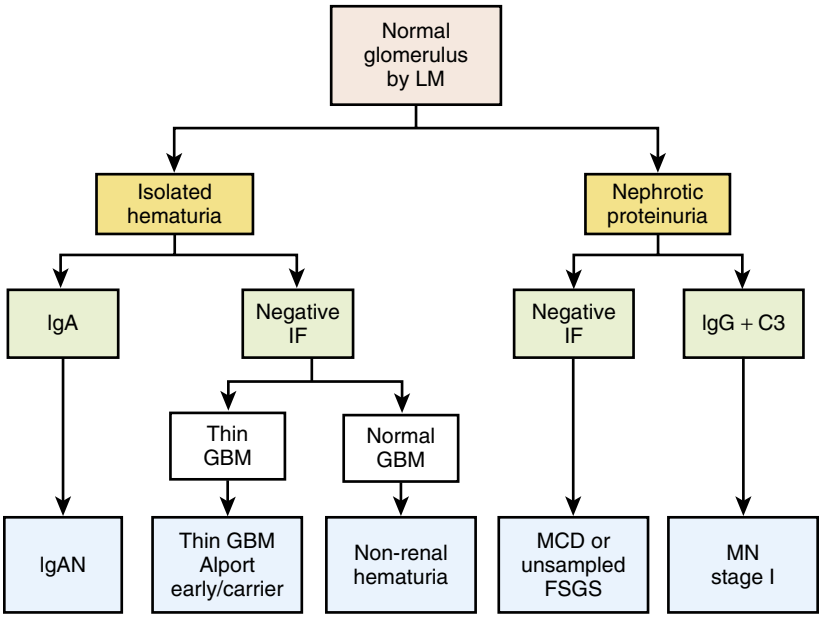

FIG. 1.1 Algorithmic approach when glomeruli appear normal by light microscopy *(LM).* Depending on the clinical setting, whether isolated hematuria or with nephrotic proteinuria, and whether immune deposits are present or not by immunofluorescence *(IF, green boxes),* varying diseases are included in the differential. These possibilities are then assessed further by electron microscopy. *FSGS,* Focal segmental glomerulosclerosis; *GBM,* glomerular basement membranes; *IgAN,* IgA nephropathy; *MCD,* minimal change disease; *MN,* membranous nephropathy.

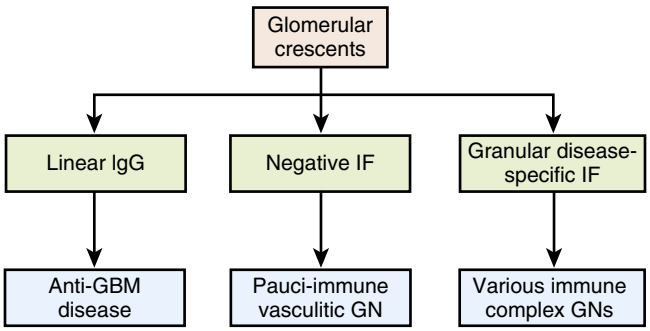

FIG. 1.2 Algorithmic approach when glomeruli show crescents by light microscopy. Depending on whether immune staining is present or not by immunofluorescence *(IF, green boxes),* and whether it is linear along glomerular basement membranes *(GBM)* or granular, varying diseases are included in the differential. *GN,* Glomerulonephritis.

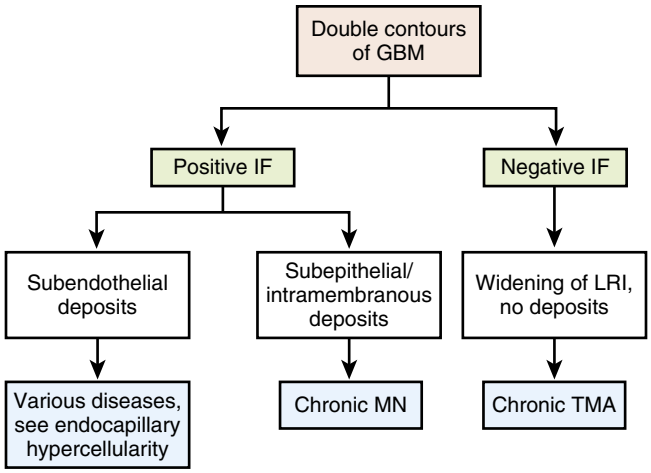

FIG. 1.3 Algorithmic approach when glomeruli show double contours of the glomerular basement membranes *(GBM)* by light microscopy. Depending on whether immune deposits are present or not by immunofluorescence *(IF, green boxes),* and specific location of deposits by electron microscopy, immune complex diseases or chronic endothelial injury (chronic thrombotic microangiopathy, *TMA*) are diagnosed. *LRI,* Lamina rara interna; *MN,* membranous nephropathy.

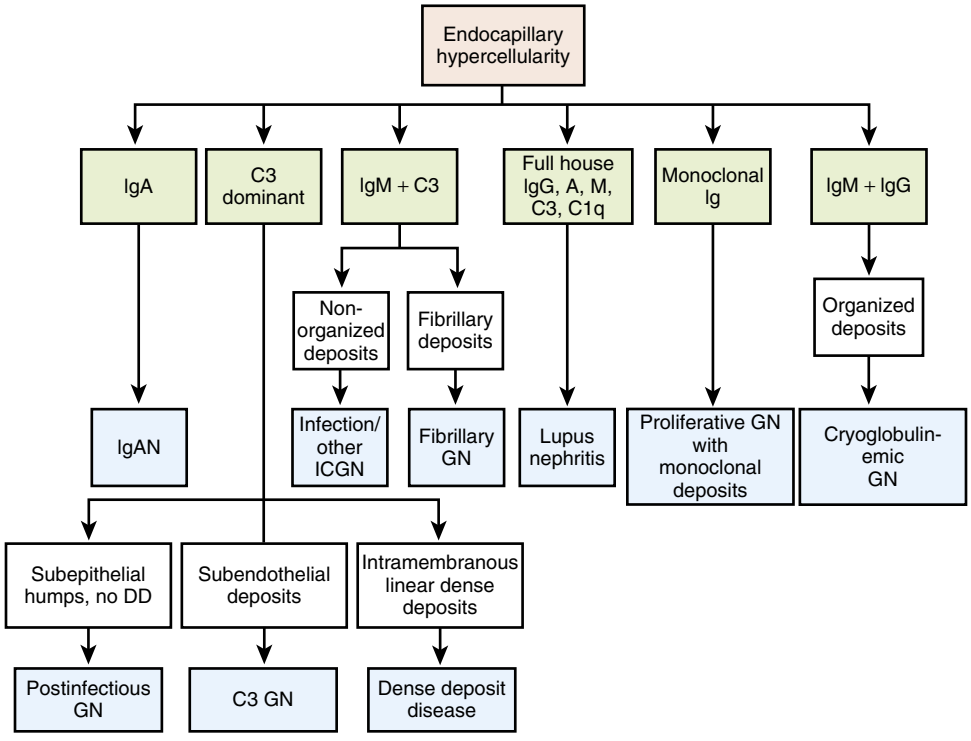

FIG. 1.4 Algorithmic approach when glomeruli show endocapillary proliferation/hypercellularity by light microscopy. Depending on the type and possible clonality of deposits by immunofluorescence *(IF, green boxes),* varying diseases are included in the differential. Electron microscopy differentiates organized versus nonorganized deposits. In the case of C3-dominant deposits, electron microscopic findings contribute to the final diagnosis. *DD,* Dense deposits; *GN,* glomerulonephritis; *ICGN,* immune complex glomerulonephritis.

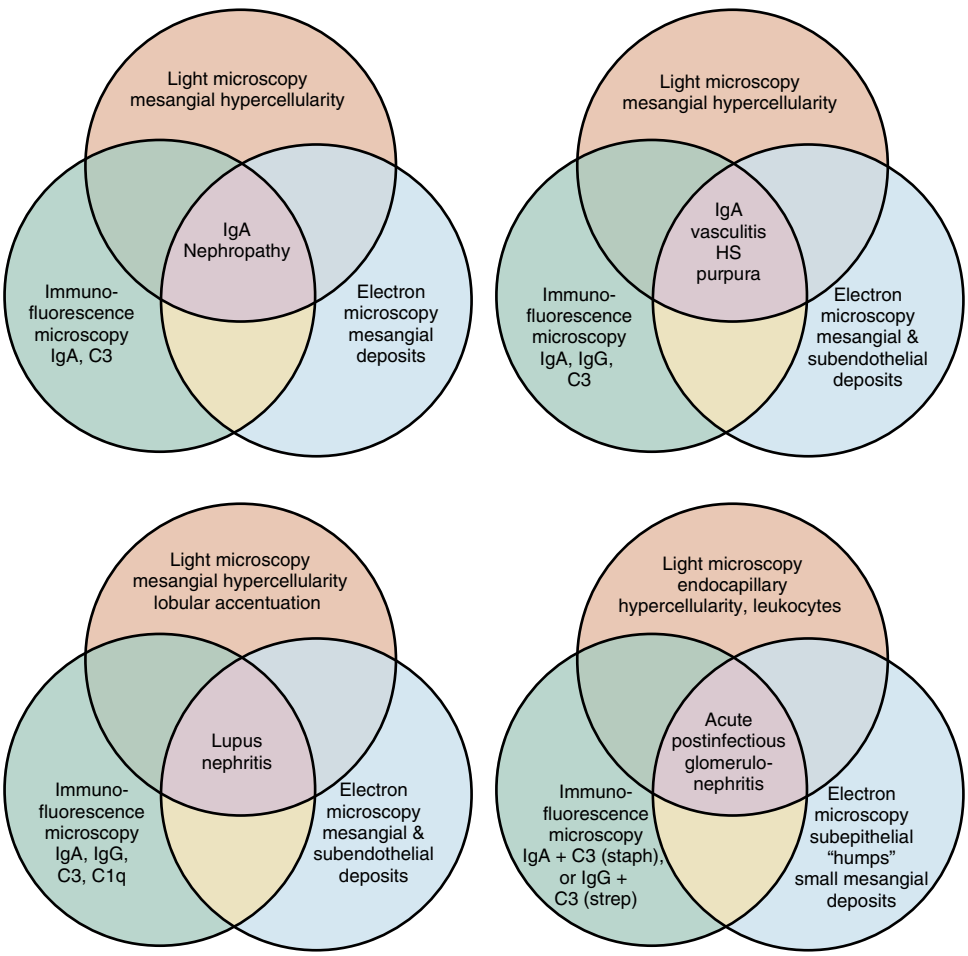

FIG. 1.5 Boolean circle analysis of glomerular lesions with IgA. The contribution of information from each of the techniques, that is, light microscopy, immunofluorescence microscopy, and electron microscopy, overlap to give the differential diagnosis by adding additional variables. *HS purpura,* Henoch–Schönlein purpura, aka IgA vasculitis.

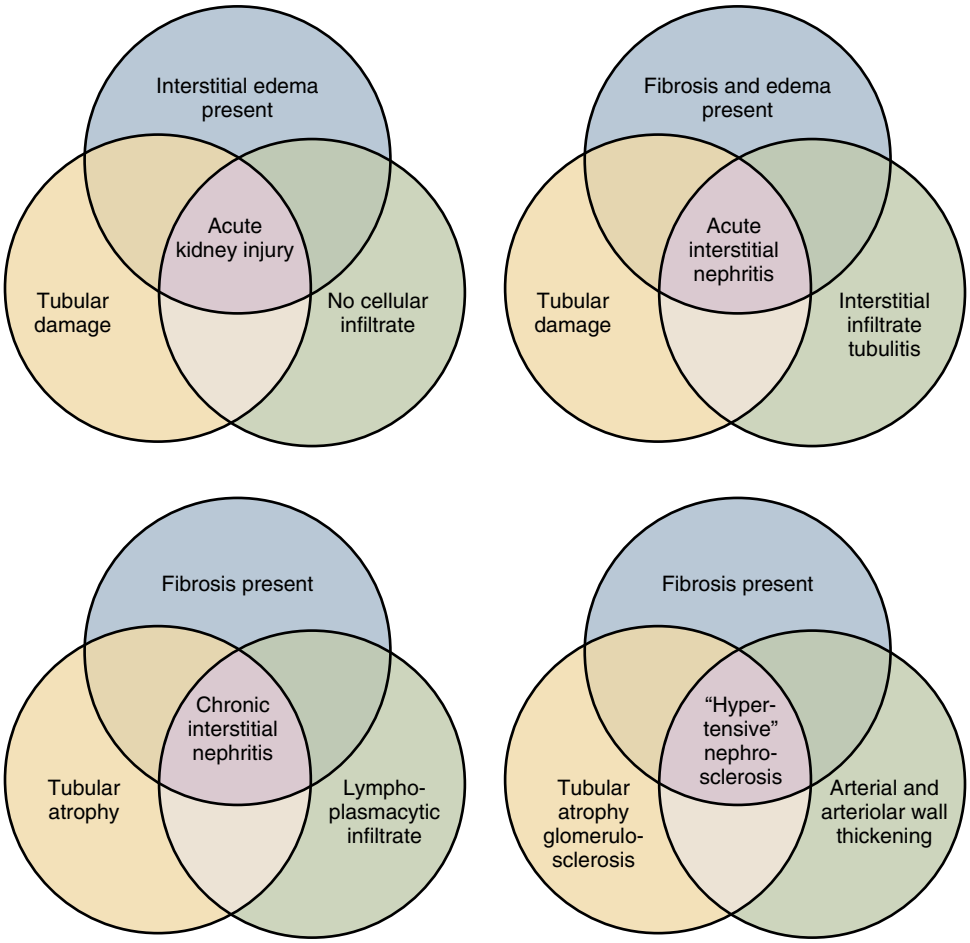

FIG. 1.6 Boolean circle analysis of tubular interstitial lesions. The contribution of information from different microscopic parameters, that is, interstitial edema or fibrosis, epithelial integrity, presence or absence of interstitial infiltrate, and vascular integrity, overlap to give the differential diagnosis by adding or deleting each of the possible variables.

TABLE 1.1 Light Microscopic Findings

Glomerular findings	
Distributional descriptors	
Focal	Involving <50% of glomeruli
Diffuse	Involving 50% or more of glomeruli
Segmental	Involving part of a glomerular tuft
Global	Involving all of a glomerular tuft
Lobular (hypersegmented)	Appearance due to endocapillary hypercellularity and consolidation of segments
Nodular	Relatively acellular, round areas of mesangial matrix expansion
Membranoproliferative	Combined capillary wall thickening with double contours and mesangial or endocapillary hypercellularity
Mesangium	Stalk region of capillary loop with mesangial cells surrounded by matrix
Lesional descriptors	
Membranous thickening	Global thickening of peripheral capillary walls with spikes
Wire loop	Thick, rigid appearance of capillary loop due to massive subendothelial deposits
Tram-track	Double contour of glomerular basement due to deposits and/or circumferential interposition
Mesangial hypercellularity	Four or more nuclei in a peripheral mesangial segment
Endocapillary hypercellularity	Increased cellularity internal to the GBM composed of leukocytes, endothelial cells, and/or mesangial cells
Extracapillary hypercellularity (crescents)	Increased cellularity in Bowman's space
Sclerosis (focal and/or segmental)	Increased extracellular matrix expanding the mesangium and obliterating capillary lumens
Necrosis	Destruction of cells and matrix with deposition of fibrin
Mesangiolysis	Loss of mesangial architecture with lysis of mesangial matrix and loss of mesangial cells
Hyaline	Glassy eosinophilic extracellular material

GBM, Glomerular basement membrane.

TABLE 1.2 Immunofluorescent Findings

Distributional descriptors for immune proteins, complement components, and fibrinogen (IgG, IgA, IgM, Kappa, Lambda, C3, C1q, C4d, Fibrinogen)
Diffuse peripheral capillary wall
Focal peripheral capillary wall
Mesangial
Peritubular
Interstitial capillary
Fluorescent patterns
Linear
Finely granular
Coarsely granular

TABLE 1.3 Electron Microscopic Findings

Capillary loops	Patent, collapsed, mesangial interposition, thrombosed
Basement membranes	Normal, thickened, attenuated, laminated, duplicated
Podocytes	Focal, segmental or global effacement, sclerotic
Endothelial cells	Fenestrations preserved, swollen, reticular inclusions Endotheliitis, lumenal leukocytes
Mesangial cells	Mild or marked increase, lysis
Mesangial matrix	Mild or marked increase, nodular, Kimmelstiel–Wilson nodules
Electron-opaque deposits	Dense, organized, granular, fibrillar, "finger print" Subepithelial and/or intramembranous ("humps") Subendothelial (occasional, numerous, paramesangial) Mesangial (occasional, abundant)
Tubules	Swollen, vacuolated, apical blebbing, apoptotic, necrosis, mitochondrial changes, epithelial detachment, deposits (powdery or dense), viral inclusions, crystals
Interstitium	Increased collagen, leukocytes, peritubular capillary multilaminated basement membranes, crystals

TABLE 1.4 Tubulointerstitial Findings

Fibrosis	Focal, diffuse, striped, percentage of sample involved
Edema	Focal, diffuse
Interstitial infiltrate	Neutrophils, eosinophils, lymphocytes, plasma cells, macrophages
Tubules	Dilated lumens, cell swelling, apical blebbing, vacuolization, flattening, cell detachment, mitosis, hyaline droplets, tubular debris atrophy, casts

TABLE 1.5 Vascular Findings

Arteries	Medial thickening, medial necrosis, mucinous degeneration, intimal proliferation, neutrophil infiltration, atheroemboli, elastin duplication
Arterioles	Intimal and medial hyalinosis, medial hyperplasia, fibrinoid necrosis, thrombosis, endotheliitis

We will elucidate the specific lesions characteristic of a range of common kidney diseases, discussed in the context of primary anatomic site of injury; that is, glomerular, vascular, and tubulointerstitial compartment. The glomerular diseases are best approached as either primary or those secondary to systemic disease, and by integrating with common clinical presentation; that is, nephrotic versus nephritic syndrome versus rapidly progressive glomerulonephritis. We will also discuss lesions in the transplant kidney, and cystic and neoplastic diseases.

Selected Reading

Sethi, S., Haas, M., Markowitz, G.S., et al., 2016. Mayo Clinic/Renal Pathology Society consensus report on pathologic classification, diagnosis, and reporting of GN. Journal of the American Society of Nephrology 27, 1278–1287.

Normal Growth and Maturation

CHAPTER 2

The normal glomerulus consists of a complex branching network of capillaries originating at the afferent arteriole and draining into the efferent arteriole (Figs. 2.1–2.3). The glomerulus contains three resident cell types: mesangial, endothelial, and epithelial. The visceral epithelial cells (also called podocytes) cover the urinary surface of the glomerular basement membrane (GBM) with foot processes, with intervening slit diaphragms. Endothelial cells are opposed to the inner surface of the GBM and are fenestrated (Figs. 2.4 and 2.5). At the stalk of the capillary, the endothelial cell is separated from the mesangial cells by the intervening mesangial matrix. The term *endocapillary* is used to describe hypercellularity/proliferation filling up the capillary lumen, contributed to by increased mesangial, endothelial, and infiltrating inflammatory cells. In contrast, extracapillary proliferation refers to proliferation of the parietal epithelial cells that line Bowman's capsule. Specific lesions are described according to

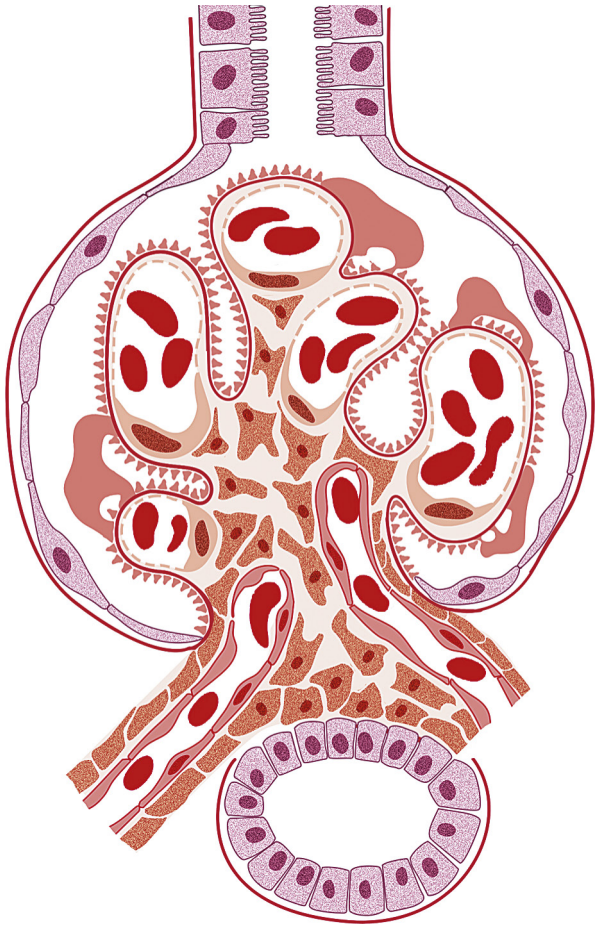

FIG. 2.1 In the normal glomerulus, the capillary loops are open, the mesangial areas have no more than three nuclei each, and foot processes are intact, without any deposits or proliferation.

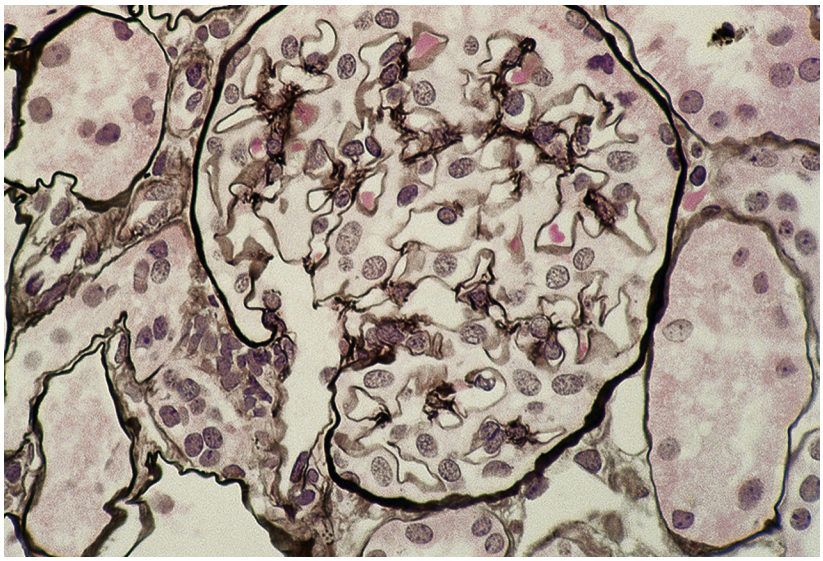

FIG. 2.2 The normal glomerulus has thin, delicate glomerular basement membranes, three or fewer mesangial cell nuclei per mesangial area, and is surrounded by Bowman's capsule. The adjacent tubules show a thin, delicate tubular basement membrane without lamellation or surrounding interstitial fibrosis. The vascular pole shows surrounding extraglomerular mesangial cells. The apparent mesangial cellularity of the glomerulus is highly dependent on the thickness of the section, and it is recommended that renal biopsies be cut at 2 μm thickness. This plastic embedded section is cut at 1 μm (Jones silver stain, ×400).

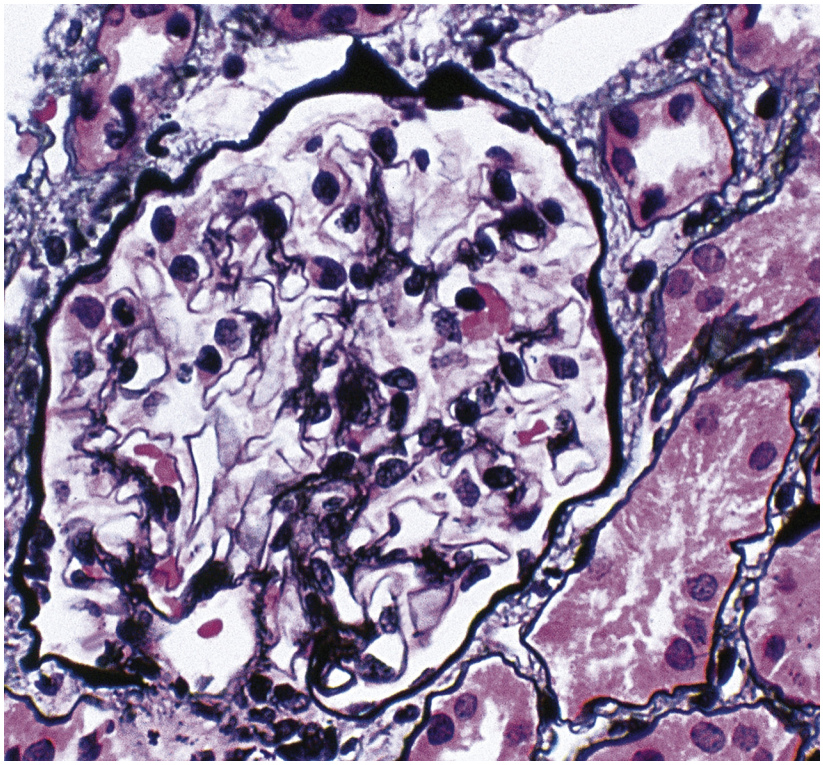

FIG. 2.3 This paraffin-embedded 2-μm section illustrates a normal glomerulus with normal vascular pole with minimal periglomerular interstitial fibrosis and surrounding intact tubules. Mesangial cellularity and matrix are within normal limits (Jones silver stain, ×400).

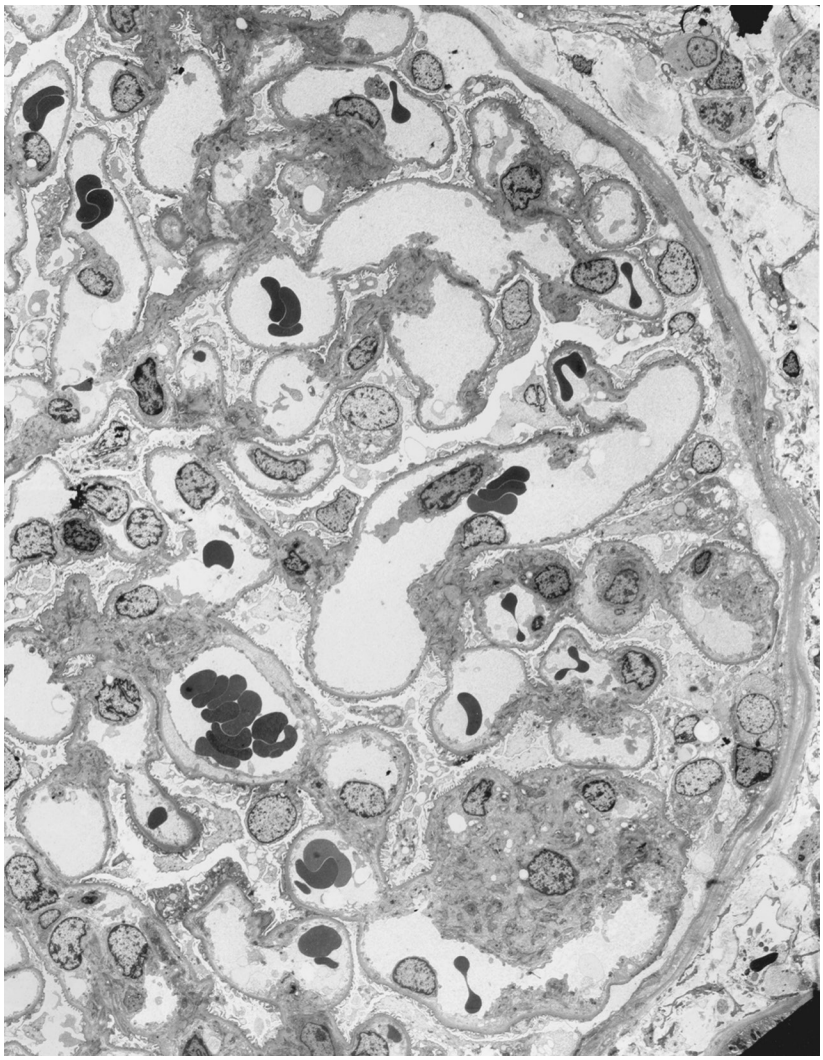

FIG. 2.4 The normal glomerular basement membrane in the adult is approximately 325–375 nm in thickness. Overlying podocytes show intact foot processes with minimal effacement in this case. The mesangial matrix surrounds mesangial cells without expansion or hypercellularity. Endothelial cells show normal fenestration. The parietal cells lining Bowman's capsule are flat and squamous in appearance (transmission electron microscopy, ×1500).

their distribution as being segmental versus global, or diffuse versus focal. Specialized terminology is also used to describe the specific lesions. A list of commonly used terms and their definitions is provided in Table 2.1.

The mesangial cell is a contractile cell that lies embedded in the mesangial matrix in the stalk region of the capillary loops, attached to anchor sites at the ends of the loop by thin extensions of its cytoplasm. Normally up to three mesangial cell nuclei are present per mesangial area. The GBM consists of three layers distinguished by electron microscopy, the central broadest lamina densa and the less electron-dense zones of lamina rara externa and interna (see Figs. 2.4 and 2.5).

The glomerulus is surrounded by Bowman's capsule, which is lined by parietal epithelial cells. These are continuous with the proximal tubule, identifiable by its periodic acid Schiff (PAS)–positive brush border. The efferent and afferent arterioles can be distinguished morphologically in favorably

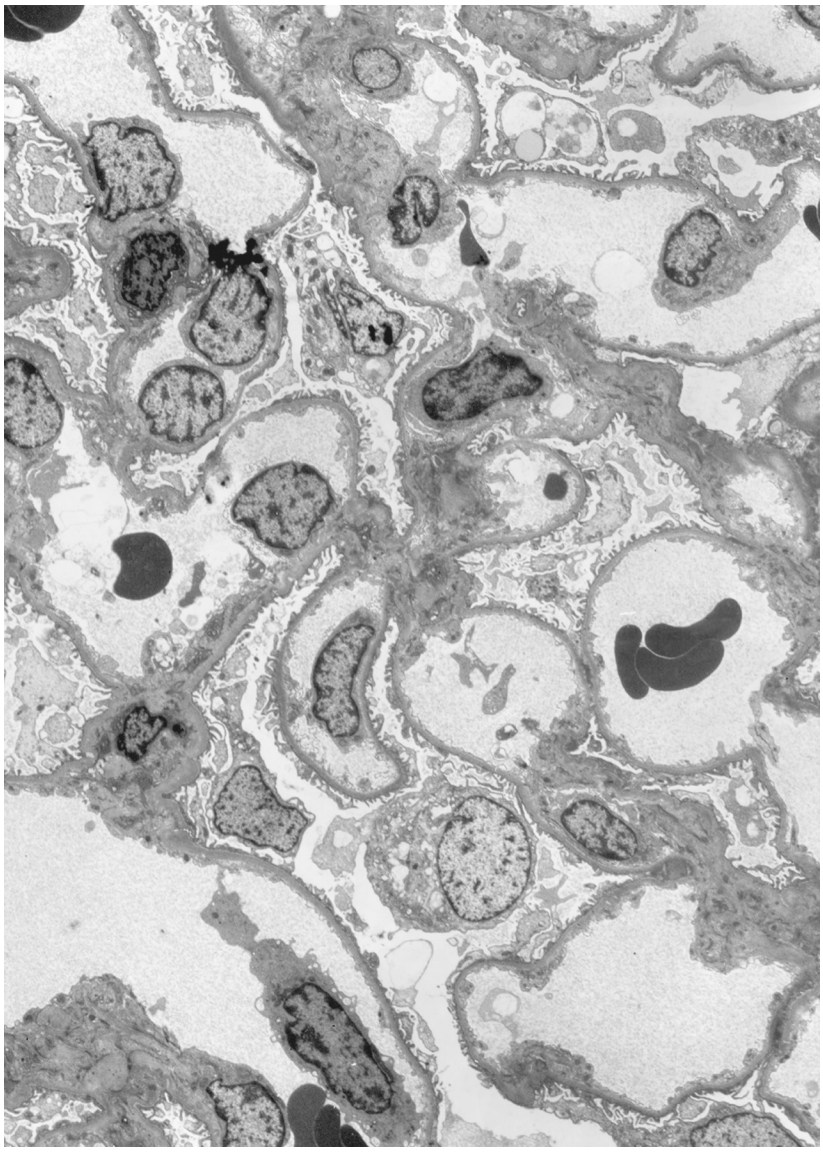

FIG. 2.5 This glomerulus shows only minimal abnormalities by electron microscopy, with rare vacuoles and blebs in the podocytes. The foot processes are largely intact. The glomerular basement membrane is of normal thickness. Red blood cells and rare platelet fragments are found within capillary lumina. The mesangial areas show mesangial cells surrounded by matrix (transmission electron microscopy, ×3000).

oriented sections or by tracing their origins on serial sections. Segmental, interlobular, and arcuate arteries may also be present in the renal biopsy specimen. The cortical biopsy also allows assessment of the tubules and interstitium. Proximal tubules are readily identified by their PAS-positive brush border, lacking in the distal tubules. Collecting ducts show cuboidal, cobblestone-like epithelium. The medulla, and even the urothelium of the calyx, may also be included in the biopsy.

During fetal maturation, the glomerular capillary tufts have a simple branching pattern with small capillary lumina and are covered by large, cuboidal, darkly staining epithelial cells (Figs. 2.6–2.8). The cells lining Bowman's space undergo change from initial tall columnar to cuboidal to flattened epithelial cells, except for those located at the opening of the proximal tubule, where cells remain taller. Immature nephrons may occasionally be seen in the superficial cortex of children up to 1 year of age

TABLE 2.1 Definitions of Common Terms to Describe Morphological Lesions

Light Microscopy	
Focal	Involving some glomeruli
Diffuse	Involving all glomeruli
Segmental	Involving part of glomerular tuft
Global	Involving total glomerular tuft
Lobular	Simplified, lobular appearance of capillary loop architecture due to endocapillary proliferation (defined below) (seen in, eg, MPGN)
Nodular	Relatively acellular areas of mesangial matrix expansion (seen in, eg, diabetic nephropathy)
Glomerular sclerosis	Obliteration of capillary loop and increased matrix
Crescent	Proliferation of parietal epithelial cells
Spikes	Projections of GBM intervening between subepithelial immune deposits (seen in, eg, membranous nephropathy)
Endocapillary proliferation	Proliferation of mesangial and/or endothelial cells and infiltrating inflammatory cells, filling up and distending capillary lumens (seen in, eg, proliferative lupus nephritis)
Hyaline	Descriptive of glassy, smooth-appearing material
Hyalinosis	Hyaline-appearing insudation of plasma proteins (seen in, eg, focal segmental glomerulosclerosis)
Mesangial area	Stalk region of capillary loop with mesangial cells surrounded by matrix
Subepithelial	Between podocyte and GBM
Subendothelial	Between endothelial cell and GBM
Tram-track	Double contour of glomerular basement due to deposits and/or circumferential interposition (see EM definitions below)
Wire loop	Thick, rigid appearance of capillary loop due to massive subendothelial deposits
Activity	Description encompassing possible treatment-sensitive lesions, eg, extent of cellular crescents, cellular infiltrate, necrosis, proliferation
Chronicity	Description of probable irreversible lesions, eg, extent of tubular atrophy, interstitial fibrosis, fibrous crescents, sclerosis
Immunofluorescence Microscopy	
Granular	Discontinuous flecks of staining producing granular pattern; seen along capillary loop in membranous nephropathy
Linear	Smooth continuous staining, seen along capillary loop in, eg, anti-GBM antibody–mediated GN, or along TBM in anti-TBM nephritis
Electron Microscopy	
Foot process effacement	Flattening of foot processes so that they cover the basement membrane, with loss of slit diaphragms
Microvillous transformation	Small extensions of visceral epithelial cells with villus-like appearance
Circumferential interposition (CIP)	Extension of mesangial cell or infiltrating monocyte cytoplasm with interposition between endothelial cell cytoplasm and basement membrane, often with underlying new basement membrane formation
Reticular aggregates	Organized arrays of membrane particles within endothelial cells (also called tubuloreticular inclusions)
Immunotactoid GP	Large, organized microtubular deposits, >30 nm diameter
Fibrillary GN	Fibrils 14–20 nm diameter without organization

EM, Electron microscopy; *GBM,* glomerular basement membrane; *GN,* glomerulonephritis; *GP,* glomerulopathy; *MPGN,* membranoproliferative glomerulonephritis; *TBM,* tubular basement membrane.

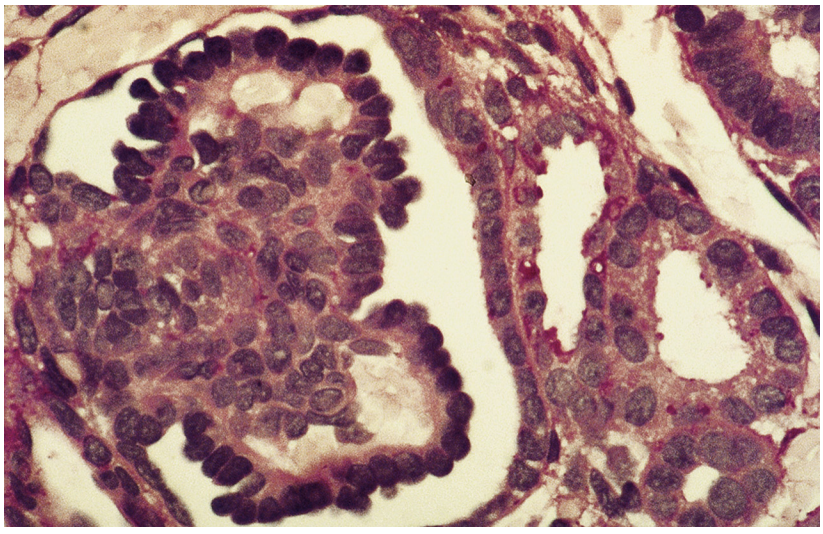

FIG. 2.6 During development, various stages of immature glomeruli may be found at different cortical levels within the kidney. The deep juxtamedullary glomeruli mature first. This immature glomerulus is from the midcortical level of a 28-week-gestation premature baby. There is prominent mesangium and very simple capillary branching with overlying plump, cuboidal glomerular visceral epithelial cells. The parietal epithelial cells lining Bowman's capsule are also more cuboidal than in the mature state (periodic acid Schiff, ×400).

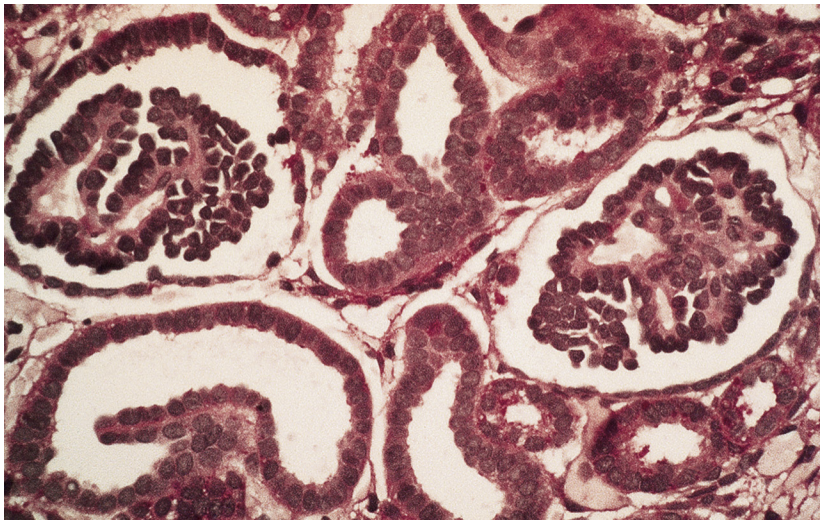

FIG. 2.7 These glomeruli are from the same 28-week-gestation baby as shown in Fig. 2.6. They have more complex capillary branching pattern but maintain immature, plump glomerular visceral epithelial cells. In one glomerulus (on the right), the parietal epithelial cells are flattened and more mature in appearance (periodic acid Schiff, ×200).

(Figs. 2.6–2.11). There is no glomerulogenesis (ie, growth of new additional glomeruli) after term birth in humans. However, increase in glomerular volume continues until adulthood, with average normal glomerular diameter approximately 95 μm in young children (average age 2.2 years) and 140–160 μm in adulthood. Thickening of the GBM also occurs normally with maturational growth. Normal ranges are from 220 to 260 nm at age 1 year, 280 to 327 nm at age 5 years, 329 to 370 nm at age 10 years, and 358 to 399 nm at age 15 years, the latter similar to adult normal thickness (see Figs. 2.4 and 2.5). Global glomerulosclerosis may occur without renal disease as a part of normal maturation, aging, and repair. Less than 5% global glomerulosclerosis is expected in children and young adults, and less than (age divided by 2, minus 10) percent in aged normal individuals.

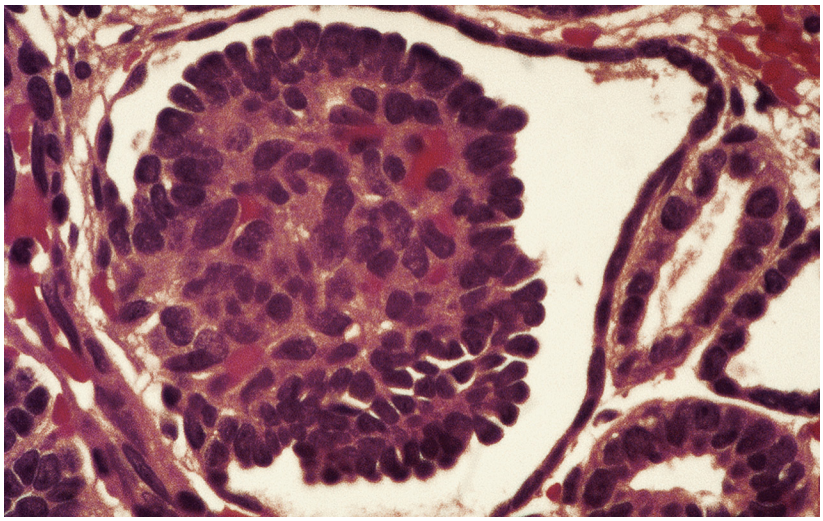

FIG. 2.8 This deep juxtamedullary glomerulus is from the same 28-week-gestation baby as shown in the previous figures. There is a complex capillary branching pattern with overlying plump, still immature glomerular visceral epithelial cells. Bowman's space is pouching out to form a junction with the proximal tubular epithelium on the right (periodic acid Schiff, ×400).

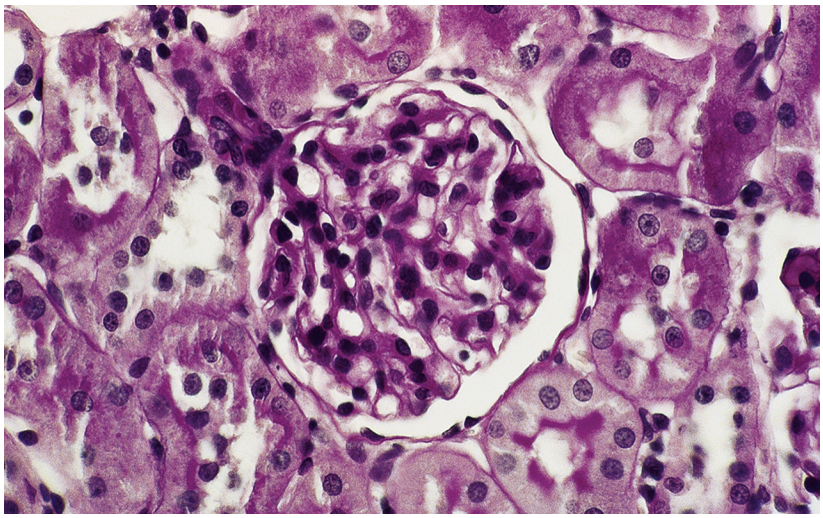

FIG. 2.9 The small but completely mature glomerulus of a normal term baby is illustrated, with complex capillary branching pattern and mature, pale-gray flattened podocytes overlying the capillary loops. The normal vascular pole is seen at the upper left. Normal proximal tubules with periodic acid Schiff–positive brush border with intervening peritubular capillaries are also illustrated. Although glomeruli do not increase in number with maturational growth, they increase in size. Normal glomerular diameter in children less than 5 years old in our biopsy practice is less than 95 μm. Individual laboratories must establish their own normal parameters because fixation and processing conditions may influence this parameter (periodic acid Schiff, ×100).

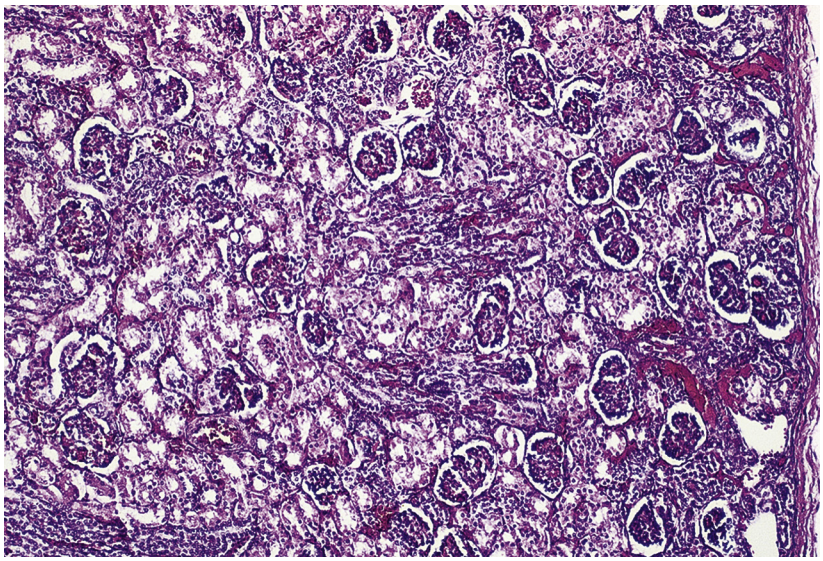

FIG. 2.10 The more superficial glomeruli *(right)* are less mature than the deeper juxtamedullary glomeruli *(left)* in this term infant. There is persistence of immature podocytes of the more superficial glomeruli, although capillary branching pattern is already complex (periodic acid Schiff, ×100).

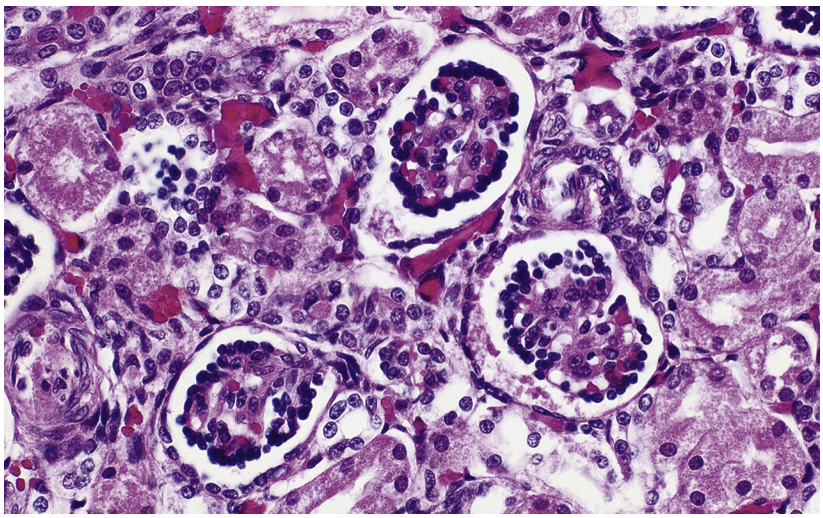

FIG. 2.11 Immature glomeruli from a 3-day-old infant show immature, plump cuboidal podocytes, with moderately complex capillary branching pattern of the glomerulus on the right, and more simple branching pattern of the glomeruli on the left (periodic acid Schiff, ×100).

Selected Reading

Fogo, A., Hawkins, E.P., Berry, P.L., et al., 1990. Glomerular hypertrophy in minimal change disease predicts subsequent progression to focal glomerular sclerosis. Kidney International 38, 115–123.

Fogo, A.B., Kon, V., 2010. The glomerulus—a view from the inside—the endothelial cell. International Journal of Biochemistry and Cell Biology 42, 1388–1397.

Kaplan, C., Pasternack, B., Shah, H., et al., 1975. Age-related incidence of sclerotic glomeruli in human kidneys. American Journal of Pathology 80, 227–234.

Kappel, B., Olsen, S., 1980. Cortical interstitial tissue and sclerosed glomeruli in the normal human kidney, related to age and sex. A quantitative study. Virchows Archiv (Pathological Anatomy) 387, 271–277.

Morita, M., White, R.H.R., Raafat, F., et al., 1988. Glomerular basement membrane thickness in children. A morphometric study. Pediatric Nephrology 2, 190–195.

Shindo, S., Yoshimoto, M., Kuriya, N., et al., 1988. Glomerular basement membrane thickness in recurrent and persistent hematuria and nephrotic syndrome: correlation with sex and age. Pediatric Nephrology 2, 196–199.

Smith, S.M., Hoy, W.E., Cobb, L., 1989. Low incidence of glomerulosclerosis in normal kidneys. Archives of Pathology and Laboratory Medicine 113, 1253–1256.

CHAPTER 3

Glomerular Diseases

Primary Glomerular Diseases

Glomerular Diseases That Cause Nephrotic Syndrome: Non-Immune Complex

MINIMAL CHANGE DISEASE AND FOCAL SEGMENTAL GLOMERULOSCLEROSIS: INTRODUCTION

Minimal change disease (MCD) and focal segmental glomerulosclerosis (FSGS) both typically present as the nephrotic syndrome and cannot be readily distinguished based solely on clinical presentation. In children ages 1–7 years, nephrotic syndrome is presumed to be due to MCD and biopsy is only done if the child is steroid unresponsive or has clinical features suggesting another etiology of the nephrotic syndrome. In adults, MCD accounts for 10–15% of nephrotic syndrome. FSGS has increased in incidence, and in the United States in adults has surpassed membranous nephropathy as a cause of nephrotic syndrome (18.7% incidence), especially in African Americans and in Hispanics. Similar increases have also been reported in children with nephrotic syndrome. Serologic studies, including complement levels, are typically within normal limits in both MCD and FSGS. Renal biopsy is thus essential to determine the etiology of nephrotic syndrome in adults, and also in children who are not steroid responders. The ultimate prognosis differs dramatically, with complete recovery the rule in MCD, contrasting with progressive renal insufficiency in FSGS. Several morphologic variants of FSGS have also been investigated for their prognostic significance. The impact of these morphologic variants on prognosis was investigated in the National Institute of Health (NIH) FSGS Clinical Trials cohort of 138 patients with steroid-resistant primary FSGS, treated with mycophenolate mofetil and dexamethasone versus cyclosporine, with no difference in response between treatment groups. However, the morphologic variant of FSGS was associated with differences in treatment responses, with worst outcome in those with collapsing variant and best in those with tip variant, with intermediate results for those with FSGS not otherwise specified (NOS). The Columbia working classification proposal is given in Table 3.1 and the hierarchical relationship of the variants is shown in Figure 3.1. Each of the subtypes will be discussed later.

MINIMAL CHANGE DISEASE

Minimal change disease (MCD) is named for the apparent structurally normal glomeruli by light microscopy (Figs. 3.2, 3.3). There are no specific vascular or tubulointerstitial lesions in idiopathic MCD. However, MCD may also occur in the middle-aged or older adult who has nonspecific focal areas of tubulointerstitial scarring and mild vascular lesions (arteriosclerosis, arteriolar hyaline related

TABLE 3.1 FSGS Variants

Type	Defining Feature
FSGS, not otherwise specified	Discrete segmental sclerosis
FSGS, perihilar variant	Perihilar sclerosis and hyalinosis
FSGS, cellular variant	Endocapillary hypercellularity
FSGS, tip variant	Sclerosis at tubular pole with adhesion at tubular lumen/neck
FSGS, collapsing variant (collapsing glomerulopathy)	Segmental or global collapse of tuft and visceral epithelial cell hyperplasia/hypertrophy

FSGS, Focal segmental glomerulosclerosis.

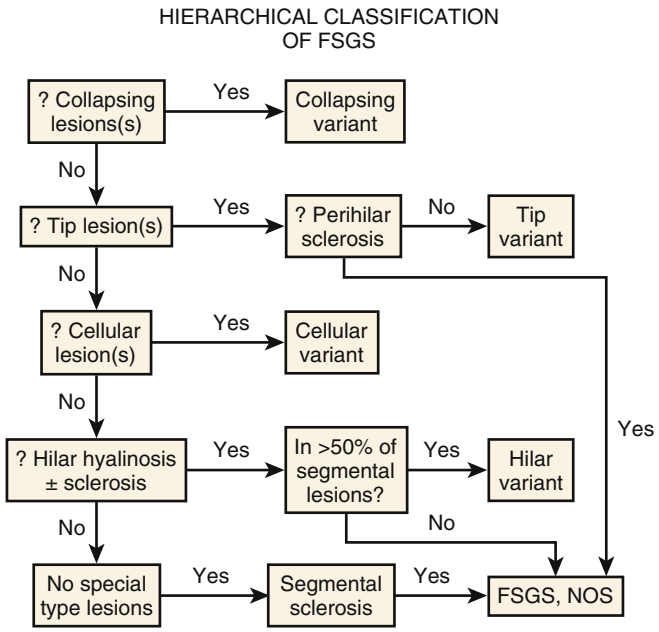

FIG. 3.1 Hierarchical classification of focal segmental glomerulosclerosis.

to hypertension, or other unrelated disease). Global glomerulosclerosis, in contrast to the segmental glomerular sclerotic lesion, is not of special diagnostic significance in considering the differential of MCD versus FSGS. Globally sclerotic glomeruli may be normally seen at any age and are thought to result from normal "wear and tear" and not specific disease mechanisms in most cases. Up to 10% of glomeruli may be normally globally sclerosed in people younger than age 40 years. The extent of global sclerosis increases with aging, up to 30% by age 80 years (estimate by calculating half the patient's age, minus 10).

Associated acute interstitial nephritis (AIN), which is characterized by edema and interstitial lymphoplasmacytic infiltrate, often with eosinophils, suggests a drug-induced hypersensitivity reaction. This combined syndrome of MCD and AIN is classically due to nonsteroidal antiinflammatory drugs (NSAIDs). This condition is usually reversible with discontinuation of the drug.

Immunofluorescence studies are typically negative in MCD. The presence of IgM staining in otherwise apparent MCD biopsies has been a source of previous controversy, with some authors considering this a specific entity, so-called IgM nephropathy (see later).

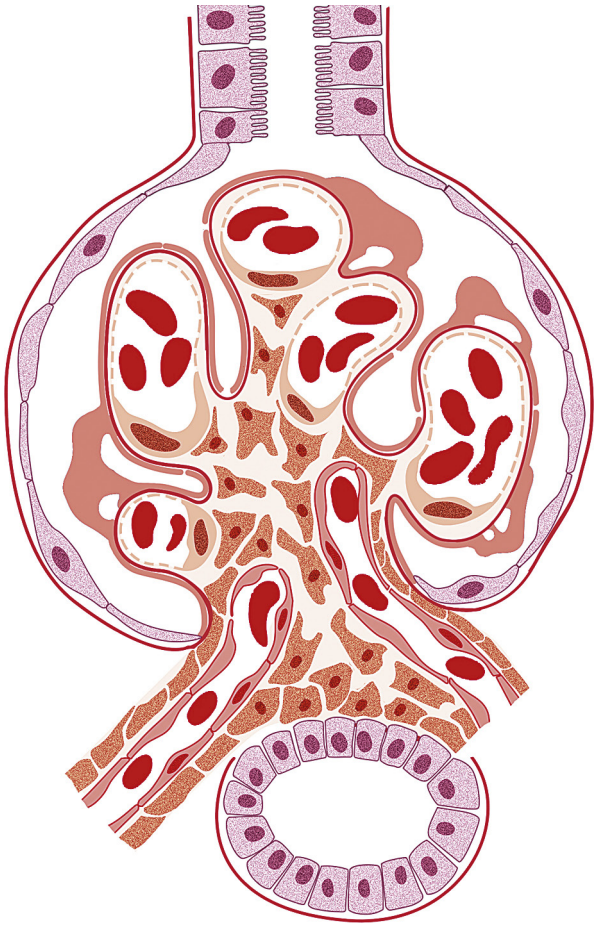

FIG. 3.2 Minimal change disease. The glomeruli are normal by light microscopy, but with diffuse effacement of foot processes by electron microscopy.

Electron microscopy (EM) shows extensive foot process effacement, vacuolization, and microvillous transformation of podocytes in MCD (Figs. 3.4, 3.5). Patients who have been treated with partial response before biopsy may show less foot process effacement.

Etiology/Pathogenesis

The pathogenesis of MCD appears related to interactions of abnormal cytokines and podocytes that only affect glomerular permeability, and do not promote sclerogenic mechanisms. Dysregulated interaction of T-cells via cytotoxic T lymphocyte antigen-4 (CTLA-4) with podocyte CD80 has been postulated, but not proven, to contribute to MCD. MCD has been associated with drug-induced hypersensitivity reactions, and can be triggered by, for example, NSAIDs (see earlier). MCD also has been associated with Hodgkin's lymphoma, bee stings, and other venom exposure and following viral infection or atopic episodes, implicating immune dysfunction as an initiating factor, but in most cases the triggers for initial disease or relapses remain unknown.

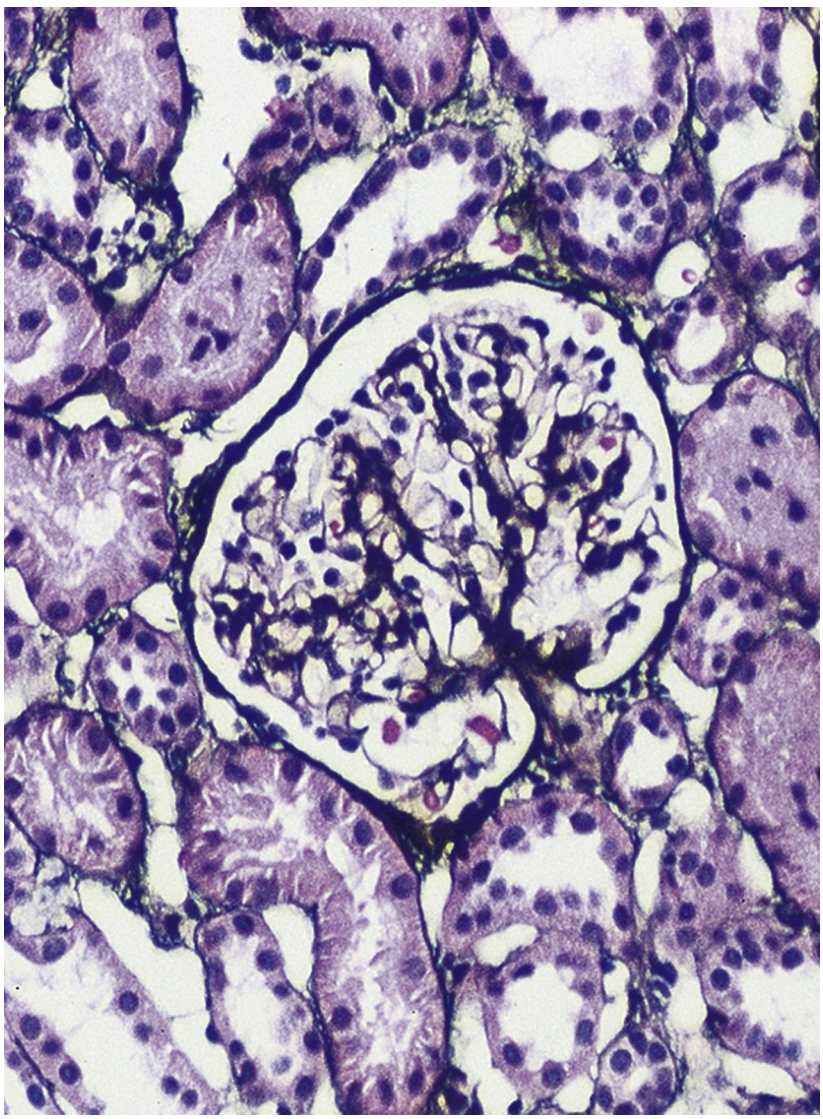

FIG. 3.3 Minimal change disease (MCD). Glomeruli appear unremarkable by light microscopy, and in young patients there is no tubulointerstitial fibrosis, as in this patient. In older patients, MCD may occur on a background of nonspecific scarring of the tubulointerstitium (Jones silver stain, ×200).

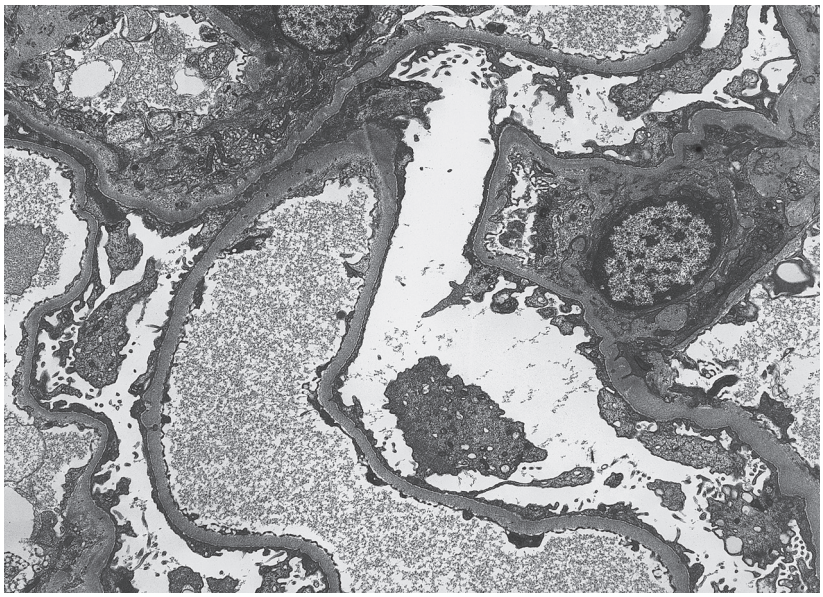

FIG. 3.4 Minimal change disease (MCD). Foot process effacement is extensive, often complete, in MCD, although extent of foot process effacement cannot be used as a definitive criterion to differentiate this entity from focal segmental glomerulosclerosis. The glomerular basement membrane is unremarkable, and there are no deposits (transmission electron microscopy, ×3000).

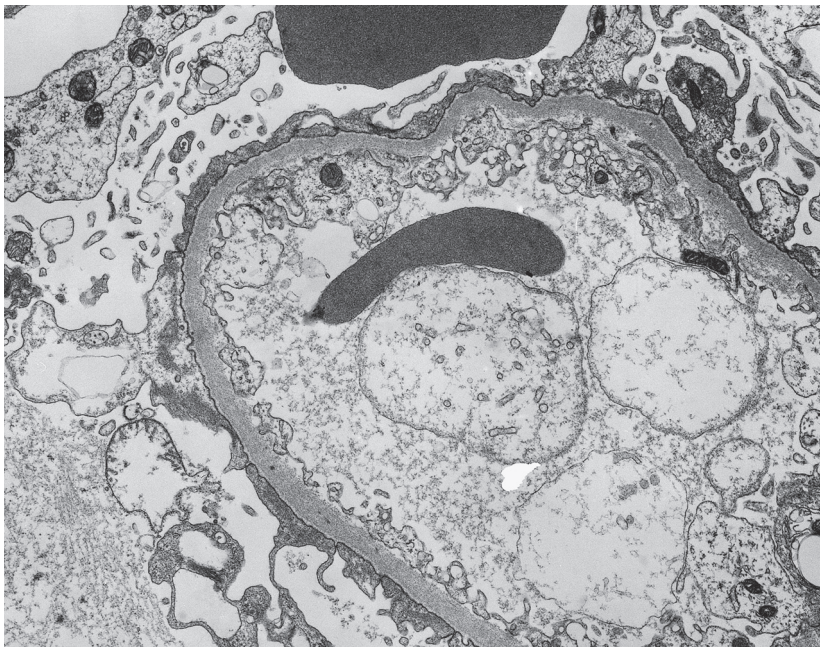

FIG. 3.5 Minimal change disease (MCD). Extensive foot process effacement and microvillous transformation of visceral epithelial cells in MCD. Although the endothelial cells are mildly swollen, the glomerular basement membrane is unremarkable, and there are no deposits (transmission electron microscopy, ×8000).

Selected Reading

Fogo, A., Ichikawa, I., 1996. Focal segmental glomerulosclerosis—a view and review. Pediatric Nephrology 10, 374–391.

Gulati, S., Sharma, A.P., Sharma, R.K., et al., 1999. Changing trends of histopathology in childhood nephrotic syndrome. American Journal of Kidney Disease 3, 646–650.

Kaneko, K., Tsuji, S., Kimata, T., Kitao, T., Yamanouchi, S., Kato, S., 2015. Pathogenesis of childhood idiopathic nephrotic syndrome: a paradigm shift from T-cells to podocytes. World Journal of Pediatrics 11, 21–28.

FOCAL SEGMENTAL GLOMERULOSCLEROSIS

In FSGS of usual type (not otherwise specified, NOS; Table 3.1), sclerosis involves some, but not all, glomeruli (focal), and the sclerosis affects a portion of, but not the entire, glomerular tuft (segmental) (Figs. 3.6, 3.7). The morphologic diagnosis of focal segmental glomerulosclerosis is a light microscopic description of this pattern of scarring, which may occur in many settings. Differentiation of MCD (see earlier) from FSGS relies on a large enough sample to detect the sclerotic glomeruli, since the detection of even a single glomerulus involved with segmental sclerosis is sufficient to invoke a diagnosis of FSGS rather than MCD. Thus, it is apparent that the distinction of MCD and FSGS may be difficult, especially with the smaller samples obtained with current biopsy guns and smaller needles. A sample of only 10 glomeruli has a 35% probability of missing a focal lesion that affects 10% of the nephrons, decreasing to 12% if 20 glomeruli are sampled. The initial sclerosis is in the juxtamedullary glomeruli, and this region

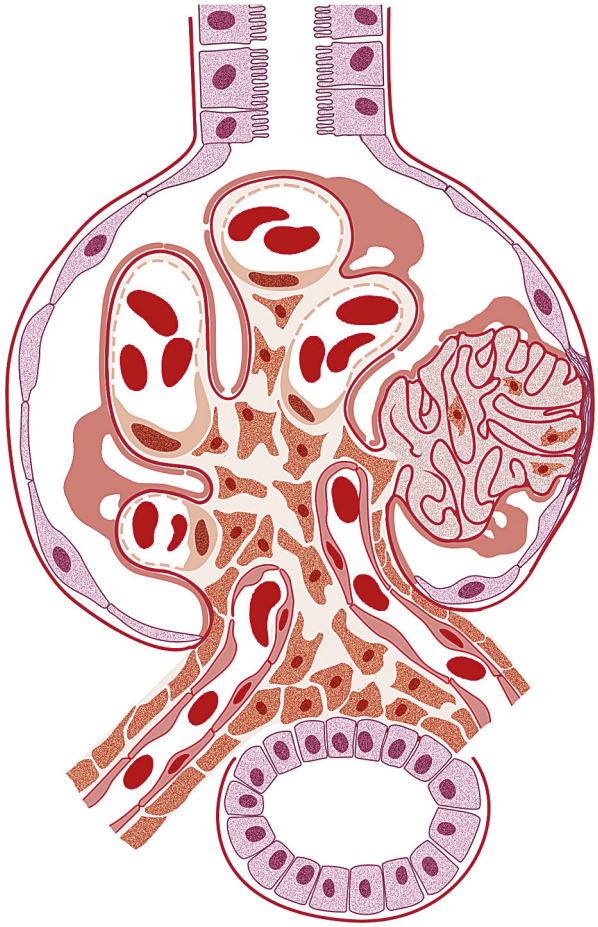

FIG. 3.6 Focal segmental glomerulosclerosis. There is sharply defined segmental sclerosis, defined as obliteration of capillary loops and increased matrix, without deposits and with diffuse foot process effacement by electron microscopy. Adhesions can also be present.

should be included in the sample (see Fig. 3.7). Conversely, sampling on one section by definition cannot identify all of the focally and segmentally distributed scars. Three-dimensional studies examining serial sections of glomeruli in cases of idiopathic FSGS have demonstrated that the process indeed is focal, that is, glomeruli without any sclerosis exist even when disease is well established (Figs. 3.8, 3.9).

Because of these limitations in detection of sclerotic lesions, other diagnostic features in glomeruli uninvolved by the sclerotic process have been sought to suspect FSGS even without sclerosed glomeruli. Abnormal glomerular enlargement (see later) appears to be an early indicator of the sclerotic process even before overt sclerosis can be detected. The presence of marked glomerular enlargement in a biopsy of

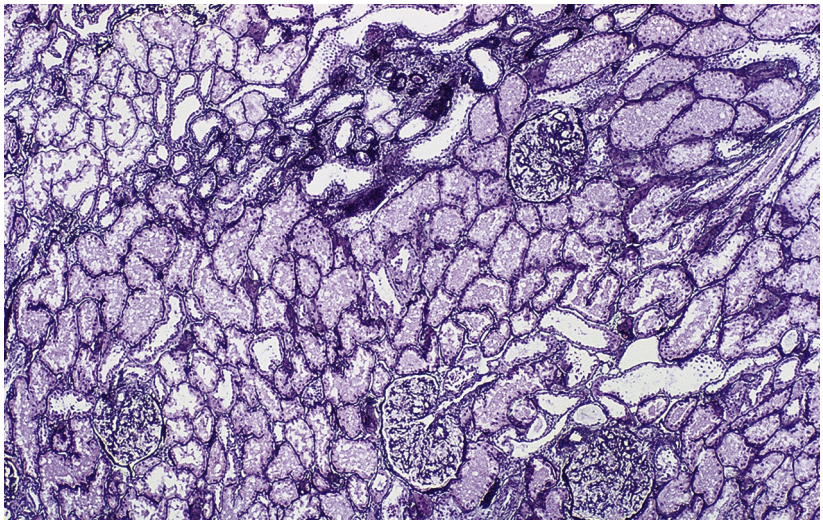

FIG. 3.7 Focal segmental glomerulosclerosis (FSGS). Early in FSGS, lesions are very focal, involving initially the juxtamedullary glomeruli. Tubulointerstitial fibrosis in a given section may be a clue to adjacent early segmental sclerotic lesions, which can be detected by careful serial section examination. In this field, one of four glomeruli *(top)* shows early segmental sclerosis of usual type, with an adjacent area of tubulointerstitial fibrosis (Jones silver stain, ×100).

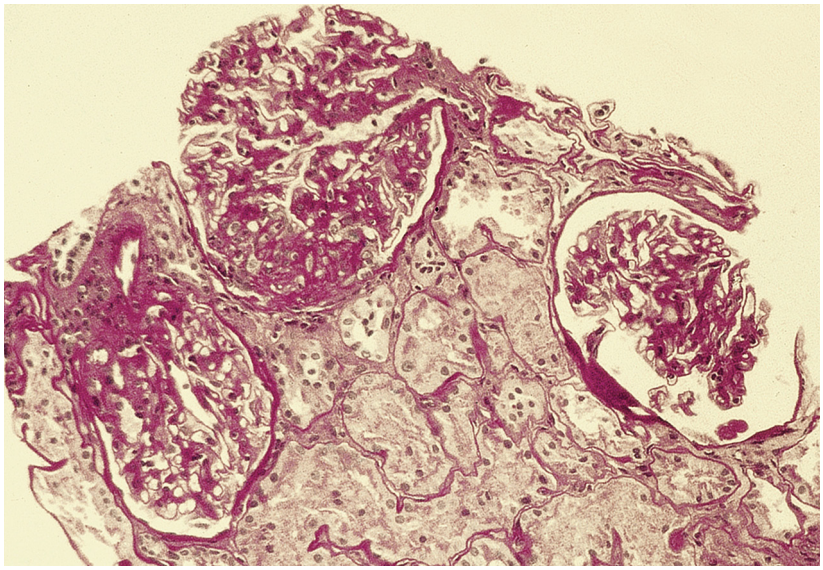

FIG. 3.8 Focal segmental glomerulosclerosis (FSGS). There is early segmental sclerosis that involves the periphery in one glomerulus *(top),* and the hilar area in another glomerulus *(left),* but without significant hyalinosis. This mixed pattern of sclerosis is characteristic of FSGS (periodic acid–Schiff, ×200).

otherwise apparent MCD would therefore rather suggest an early, incipient stage of FSGS. Dystroglycan, a component of normal glomerular basement membrane (GBM) that contributes to podocyte–matrix interaction, is generally maintained in nonsclerotic segments in FSGS, and decreased in MCD (but also in collapsing type FSGS). This marker, or other emerging biomarkers from molecular and proteomic studies, while not completely sensitive or specific, may be of aid in favoring unsampled FSGS versus MCD in a biopsy with extensive foot process effacement and no defining segmental lesion. Diffuse mesangial hypercellularity may be a morphologic feature superimposed on changes of either MCD or FSGS, with or without IgM deposits, without defined prognostic significance (see later).

The periodic acid–Schiff (PAS)-positive acellular material in the segmental sclerotic lesions of the glomerulus may have different composition depending on the diverse pathophysiologic mechanisms discussed later. The sclerotic process is defined by glomerular capillary obliteration with increase in matrix, and varies from small, early lesions to near global sclerosis (Figs. 3.10–3.13). The segmental sclerosis lesions are discrete and may be located in perihilar and/or peripheral portions of the glomerulus. There may be associated global glomerulosclerosis, which has no specific diagnostic significance. Uninvolved glomeruli show no apparent lesions by light microscopy, but may appear enlarged, as do glomeruli with early-stage segmental sclerosis. The glomerulosclerosis may be associated with hyalinosis, resulting from insudation of plasma proteins, producing a smooth, glassy (hyaline) appearance (Fig. 3.14). This occurs particularly in the axial, vascular pole region. Of note, arteriolar hyalinosis may occur with hypertensive injury and should not be taken per se as evidence of a glomerular sclerotic lesion (see hilar-type FSGS, discussed later). Vascular sclerosis may be prominent late in the course of FSGS. Adhesion of the podocyte to Bowman's capsule (synechiae) is an early manifestation of sclerosis (Fig. 3.15). Glomerulosclerosis, when fully established, is accompanied by tubular atrophy, interstitial fibrosis with interstitial lymphocytes, proportional to the degree of scarring in the glomerulus (see Fig. 3.11). Of note, in HIV-associated nephropathy (HIVAN) and collapsing glomerulopathy, tubular lesions are often microcystic and disproportionally severe (see later).

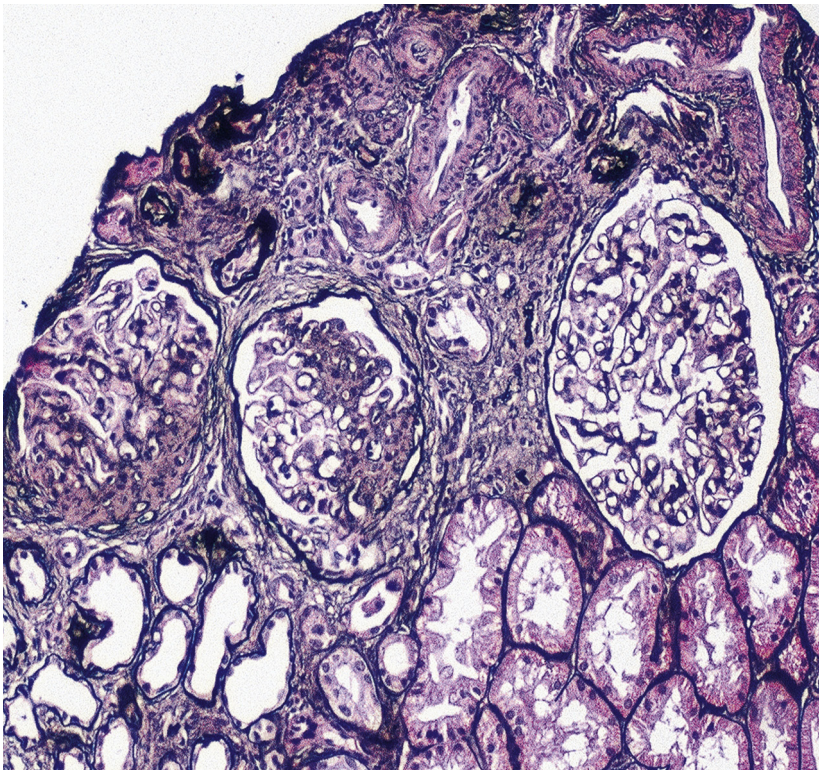

FIG. 3.9 Focal segmental glomerulosclerosis (FSGS). There are more advanced segmental sclerotic lesions affecting two of the three glomeruli in this field, with surrounding proportionate tubulointerstitial fibrosis. The sclerosis is characterized by increased matrix and obliteration of capillary lumens, and is of the usual type of FSGS (Jones silver stain, ×200).

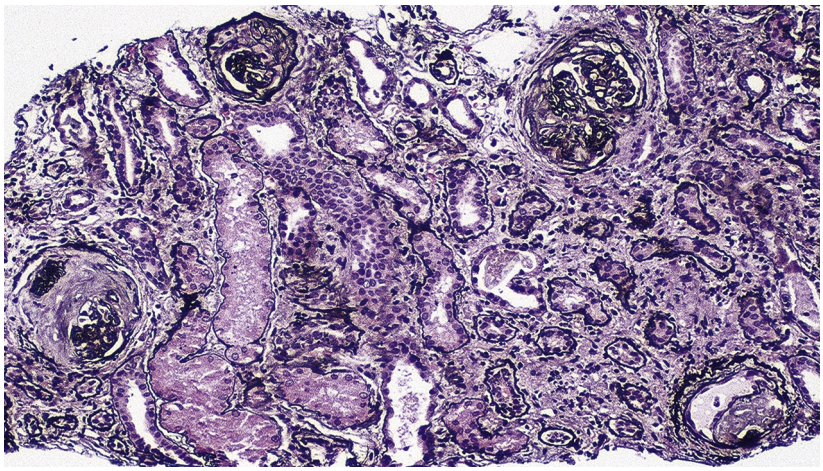

FIG. 3.10 Focal segmental glomerulosclerosis (FSGS). Near end-stage FSGS is present, with global or near global sclerosis of all glomeruli and extensive tubulointerstitial fibrosis and vascular thickening (Jones silver stain, ×200).

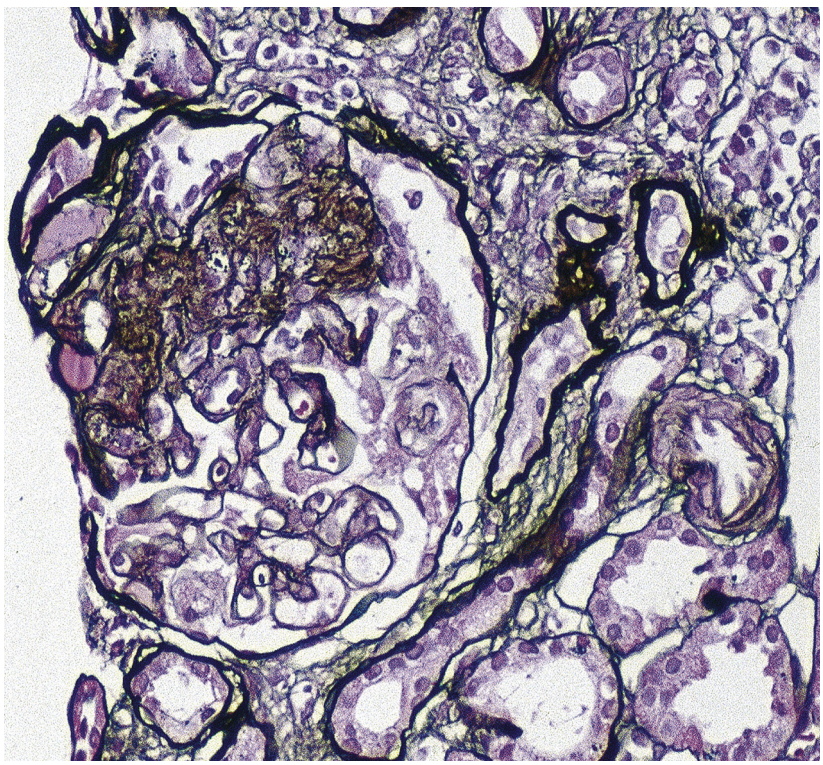

FIG. 3.11 Focal segmental glomerulosclerosis (FSGS). The typical segmental sclerotic lesion in FSGS is characterized by increased matrix and obliteration of capillary lumina, frequently with hyalinosis and adhesions, as illustrated here. There is surrounding tubulointerstitial fibrosis. The uninvolved segment of the glomerulus appears unremarkable (Jones silver stain, ×200).

Immunofluorescence may show nonspecific entrapment of IgM and C3 in sclerotic areas or areas where the mesangial matrix is increased (Fig. 3.16).

Electron microscopy shows extensive foot process effacement, even in glomeruli without a segmental sclerosing lesion (Fig. 3.17). Thus, extent of foot process effacement does not allow precise distinction between MCD and FSGS in individual cases. Foot process effacement tends to be more extensive in primary FSGS compared with secondary FSGS; however, the overlap between these two categories does not allow one to use this as a diagnostic feature in individual cases. Secondary FSGS lesions may show extensive foot process effacement in glomeruli affected by the segmental sclerosing process. Conversely, the absence of significant, that is, less than 50%, foot process effacement should cast doubt on the diagnosis of primary, idiopathic FSGS. There are no immune deposits in idiopathic FSGS, but mesangial matrix is increased in sclerotic areas (Fig. 3.18). Areas of hyalin may be present in the sclerotic segments and appear dense by electron microscopy, but should be readily recognized as hyaline, and not confused with immune complexes, by observing scattered lipid droplets, and correlating with scout section light microscopic appearance (Fig. 3.19). The presence of numerous reticular aggregates in endothelial cells in the setting of segmental glomerulosclerosis with collapsing features suggests possible HIV-associated nephropathy (see later).

Diagnosis of Recurrence of FSGS in the Transplant

Primary FSGS recurs in 30–40% of patients. Most recurrences occur within the first months after transplantation, although proteinuria may recur immediately after the graft is implanted, implicating circulating factor(s) in the recurrence. Foot process effacement is present at time of recurrence of proteinuria and precedes the development of sclerosis, typically by weeks to months. Glomerular enlargement at this stage of recurrent FSGS is prominent in children, who otherwise do not undergo glomerular enlargement when receiving an adult kidney (in contrast, an adult recipient of a single kidney will normally have marked renal and glomerular growth to provide adequate glomerular filtration

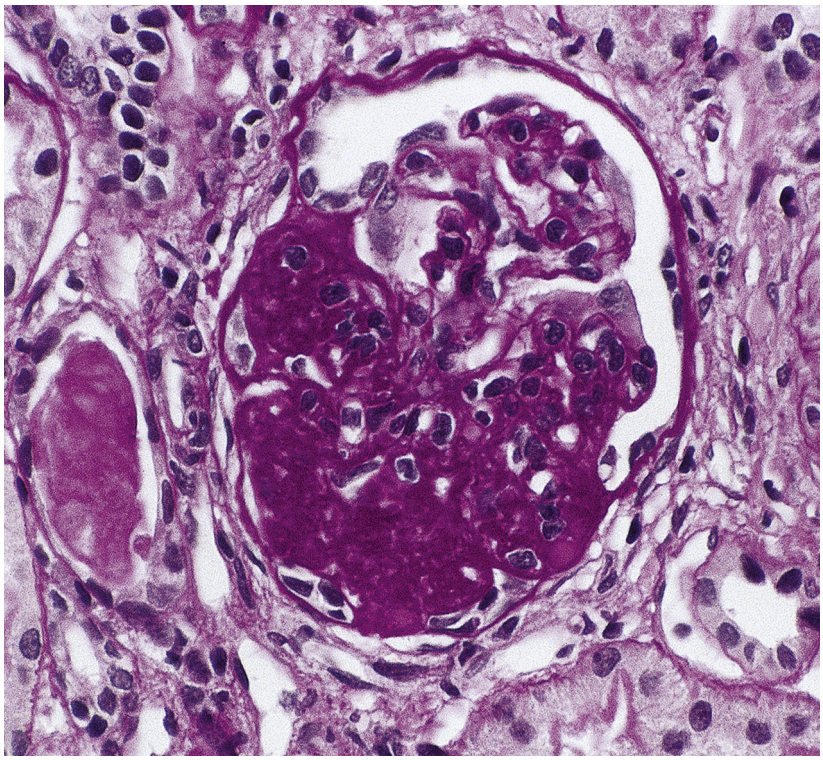

FIG. 3.12 Focal segmental glomerulosclerosis (FSGS). An advanced segmental sclerotic lesion of FSGS is shown, with only minimal hyaline droplets. There is increased mesangial matrix and obliteration of capillary lumina involving the majority of the glomerulus. The uninvolved portion of the glomerulus has mild increase in mesangial matrix. The adjacent tubule shows atrophy and a proteinaceous cast (periodic acid–Schiff, ×400).

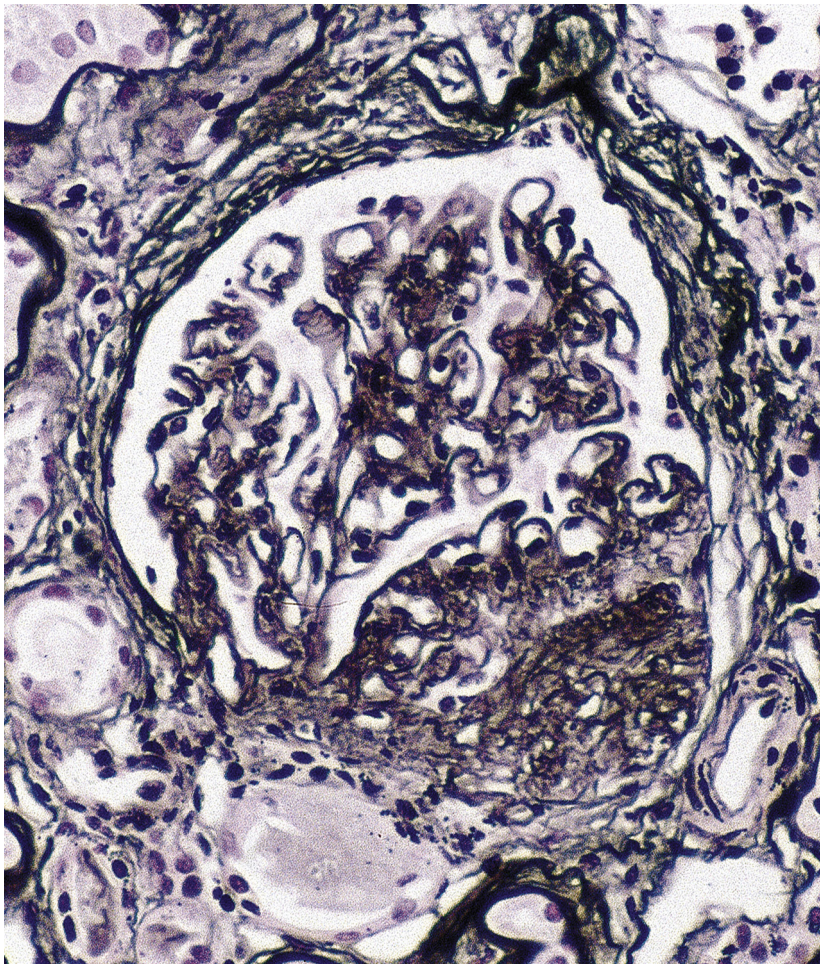

FIG. 3.13 Focal segmental glomerulosclerosis (FSGS). The segmental sclerotic lesion of FSGS is illustrated, with increased mesangial matrix and obliteration of capillary lumina. The remnants of the glomerular basement membrane in the sclerosed segment can be seen as wrinkled lines on this silver stain. The uninvolved portion of the glomerulus shows minimal mesangial matrix increase. Although this sclerotic lesion involves the vascular pole, there is no associated hyalinosis, and the majority of segmental lesions were not hilar, the lesion is therefore classified as FSGS, not otherwise specified (Jones silver stain, ×400).

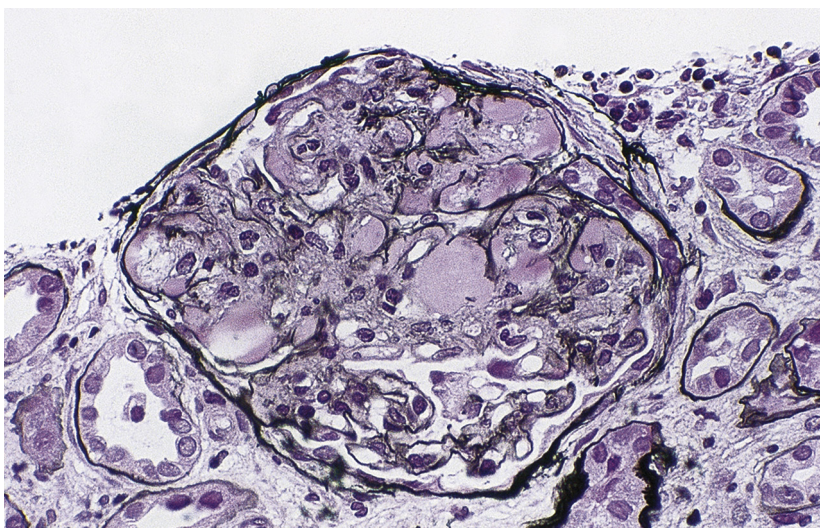

FIG. 3.14 Focal segmental glomerulosclerosis (FSGS). In this case of FSGS, there was extensive hyalinosis in the sclerotic areas, which are characterized by increased mesangial matrix and obliteration of capillary lumina. There are also adhesions of the sclerotic segments to Bowman's capsule, with thickened and disrupted Bowman's capsule. The hyalinosis represents an insudation of plasma proteins, reflecting endothelial injury (Jones silver stain, ×400).

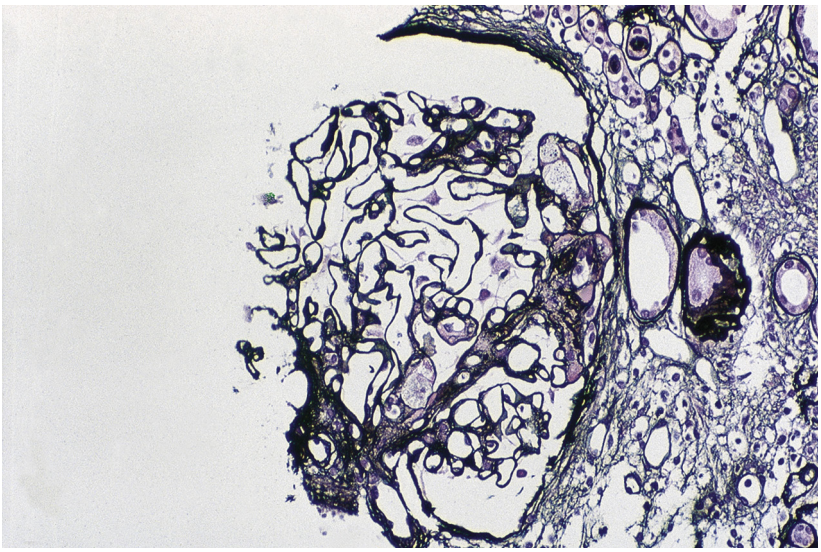

FIG. 3.15 Focal segmental glomerulosclerosis (FSGS). Early lesion of FSGS with adhesion of glomerular tuft to Bowman's capsule and small segmental area of hyalinosis and intracapillary foam cells (Jones silver stain, ×400).

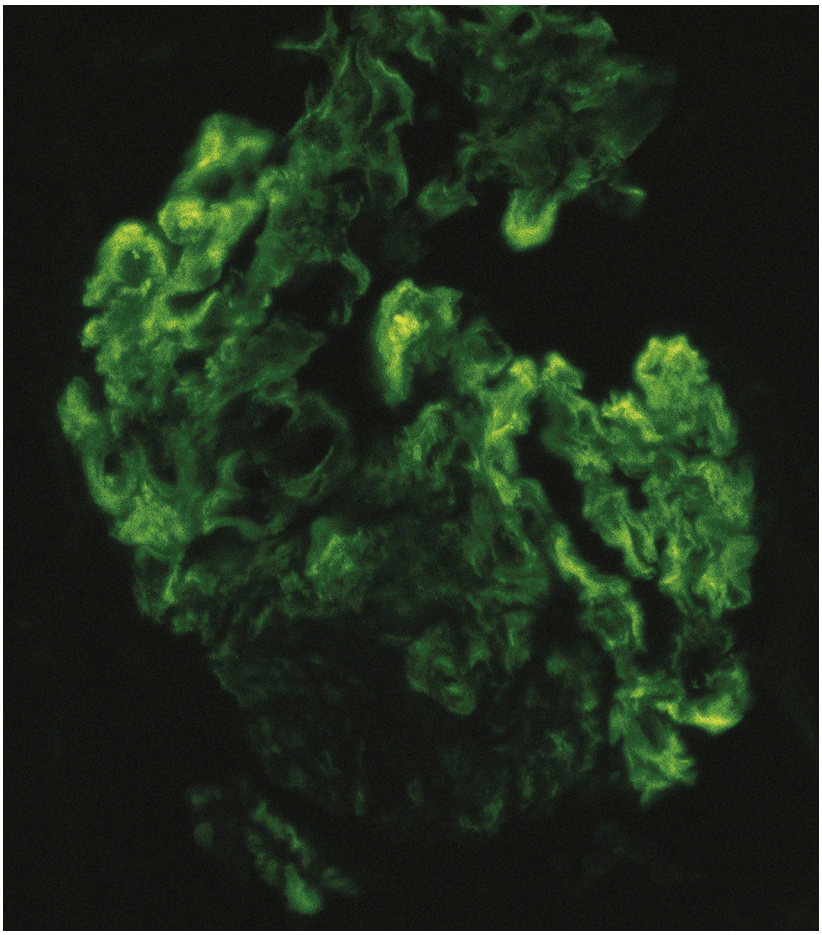

FIG. 3.16 Focal segmental glomerulosclerosis (FSGS). Immunofluorescence studies in FSGS do not show immune complexes, but may show IgM in sclerotic areas or in areas of mesangial expansion (anti-IgM antibody immunofluorescence, ×400).

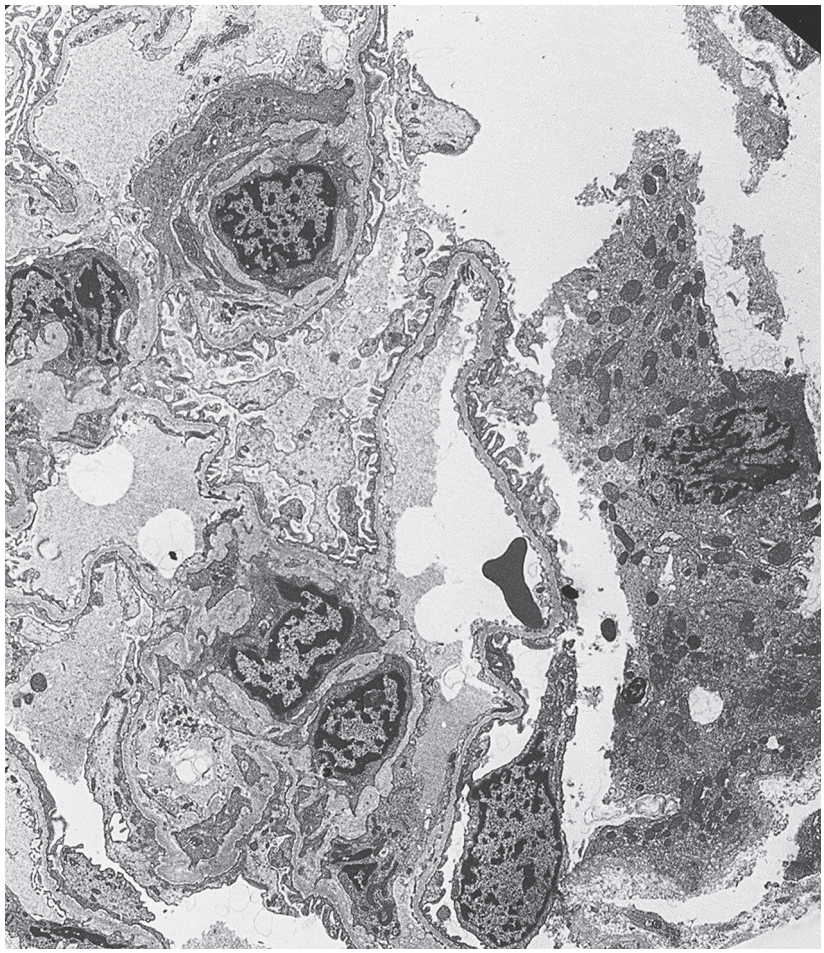

FIG. 3.17 Focal segmental glomerulosclerosis (FSGS). By electron microscopy, there is extensive foot process effacement in FSGS. However, it may not be complete, as illustrated here. If there is less than approximately 50% foot process effacement, the diagnosis of primary FSGS is in doubt. There is also mesangial matrix expansion, without immune deposits (transmission electron microscopy, ×3000).

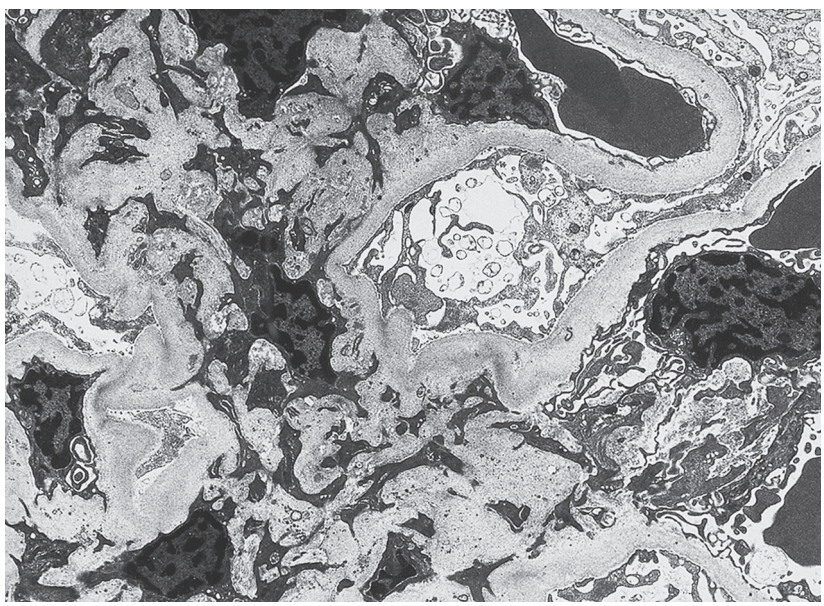

FIG. 3.18 Focal segmental glomerulosclerosis (FSGS). Segmental increase in matrix with obliterated capillary lumens is apparent in this case of FSGS. The overlying visceral epithelial cells show vacuolization, microvillous transformation, and extensive foot process effacement. The corrugated, collapsed glomerular basement membrane is evident. There are no immune deposits (transmission electron microscopy, ×5000).

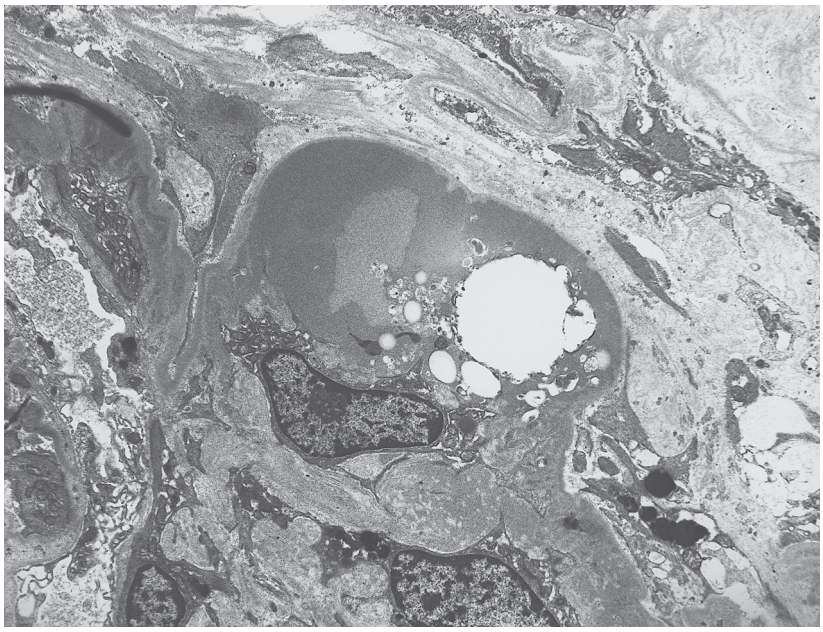

FIG. 3.19 Focal segmental glomerulosclerosis (FSGS). Hyaline deposit within a segmentally sclerotic area in FSGS. Hyaline is smooth, homogeneous, usually located in areas of sclerosis, and frequently contains lipid (clear, round areas). The sclerotic segment is characterized by increased matrix and obliteration of the capillary lumen, with dense adhesion to the overlying fibrotic Bowman's capsule (transmission electron microscopy, ×3000).

rate [GFR]). Overt sclerosis is not noted until weeks to even months after recurrence of nephrotic syndrome. Thus, during this time interval in the setting of the FSGS patient with nephrotic syndrome in the transplant, foot process effacement alone, even without detectable segmental sclerosis, is evidence of recurrent FSGS. Activated parietal epithelial cells, staining for CD44, are increased on the glomerular tuft itself even in this early phase of recurrent FSGS, and are postulated to have migrated from Bowman's capsule. Recurrent FSGS often, but not invariably, shows similar phenotype by the Columbia classification of FSGS as in the native kidney.

Differential Diagnosis of MCD Versus FSGS

Some investigators have felt that the common clinical presentation and similar findings in intact glomeruli indicate that MCD and FSGS are two manifestations of the same disease. Our data and those from others rather support differences even at the earliest time points. Much evidence has pointed to the participation of abnormal glomerular adaptation and growth factors in the pathogenesis of glomerulosclerosis. Several studies have shown that glomerular enlargement precedes overt glomerulosclerosis, in both pediatric and adult patients who otherwise had apparent MCD initially. Patients with abnormal glomerular growth, even on initial biopsies that did not show overt sclerotic lesions, subsequently developed overt glomerulosclerosis, as documented in later biopsies. A cut-off of >50% larger glomerular area than normal for age was a sensitive indicator of increased risk for progression in one series of children with nephrotic syndrome. Of note, glomeruli grow in size until approximately age 18 years, although no new glomeruli are formed after birth, so age-matched controls must be used in the pediatric population to assess normal glomerular size.

The finding of mesangial hypercellularity (>80% of glomeruli with >3 cells per mesangial region) has been proposed to indicate a subgroup of patients with poorer prognosis and increased risk for development of FSGS. Lack of uniform application of criteria for morphologic definition of mesangial hypercellularity makes it difficult to assess the impact of this feature on prognosis. However, several series have failed to confirm a definite clinical correlation of this morphologic variant. Thus, patients with mesangial hypercellularity in renal biopsies that otherwise show apparent MCD ultimately had good prognosis despite decreased initial response to

Continued